Available online at www.sciencedirect.com

SCIENCE DIRECT®

Geomorphology 64 (2005) 133–166

GEOMORPHOLOGY

www.elsevier.com/locate/geomorph

Shelf-edge deltas and drowned barrier–island complexes on the northwest Florida outer continental shelf

J.V. Gardner[a,*], P. Dartnell[a], L.A. Mayer[b], J.E. Hughes Clarke[c], B.R. Calder[b], G. Duffy[c]

[a]*U.S. Geological Survey, Menlo Park, CA 94025, USA*
[b]*University of New Hampshire, Durham, NH 03824, USA*
[c]*University of New Brunswick, Fredericton, NB E3B 583, Canada*

Received 18 November 2003; received in revised form 3 June 2004; accepted 4 June 2004
Available online 17 August 2004

Abstract

A high-resolution multibeam survey of the northwest Florida shelf mapped six relict shelf-edge deltas, each with a drowned barrier–island system developed on its south and southwestern rims. The deltas appear to have formed during periods of sea-level stasis that occurred between 58,000 and 28,000 years ago. The barrier islands formed on the deltas during periods of slow regression during this same time interval. Large fields of asymmetric dunes are found on the delta surfaces as well as on the south and southwestern flanks of the deltas. The asymmetry and orientation of the dunes suggest that a northward-flowing current was sheared by the presence of the delta topography, and as a result, the upper layer of the flow continued to the north, whereas the lower layer was steered by the topography. The topographic steering accelerated the northward flow around the south and southwestern flanks with speeds adequate to form large dunes. The flow slowed after rounding southwestern flank but accelerated again as it encountered the next delta flank to the north. The age of the dune formation is unknown, and no northward-flowing geostrophic flow has been reported in the literature from this area.

Keywords: Gulf of Mexico; Barrier islands; Sea level; Shelf-edge deltas; Bed forms

1. Introduction

A large contiguous area of the mid- and outer continental shelf off NW Florida was mapped using a high-resolution multibeam echosounder (MBES) to map the detailed geomorphology of the area bounded by the 40- and 150-m isobaths from immediately south of the head of De Soto Canyon (30°00′ N 86°39′ W) along an SE-trending corridor to 28°56′ N

* Corresponding author. Current address: Center for Coastal and Ocean Mapping, University of New Hampshire, 24 Colovos Road, Durham, NH 03824, USA. Tel.: +1 603 862 3473; fax: +1 603 862 0839.

E-mail addresses: jim.gardner@unh.edu (J.V. Gardner), pdartnell@usgs.gov (P. Dartnell), larry.mayer@unh.edu (L.A. Mayer), jhc@omg.unb.ca (J.E. Hughes Clarke), bcalder@cisunix.unh.edu (B.R. Calder), gduffy@omg.unb.ca (G. Duffy).

0169-555X/$ - see front matter © 2004 Elsevier B.V. All rights reserved.
doi:10.1016/j.geomorph.2004.06.005

85°25′ W (Fig. 1). An additional area was mapped that is bounded by 28°03′ N to 28°14′ N and 84°37′ W to 84°48′ W. The objectives of this paper are to describe the geomorphology of the areas mapped and to speculate on the processes that formed the features. The focus is on a series of relict shelf-edge deltas, barrier islands, and large bed forms.

1.1. Mapping systems

A Kongsberg Simrad EM1002 MBES was used to map the areas. An overview of high-resolution MBES systems can be found in Hughes Clarke et al. (1996) and Hughes Clarke (2000), and details of the EM1002 can be found in Gardner et al. (2002). Navigation for the cruise was with a DGPS-aided inertial system that provided spatial accuracies of ±0.5 m; depth accuracy is better than 0.5% of the water depth. The 95-kHz EM1002 MBES not only provides hydrographic-quality bathymetry but also generates "quantitative" seafloor acoustic backscatter data that can be displayed as a side-scan sonar-like image. If properly calibrated, and bed roughness and volume reverberation are ignored, the acoustic backscatter values can be directly compared to empirical correlations of backscatter versus grain size (Jackson, 1994; Table 1). The backscatter data are used to gain insights into the spatial distribution of the geological properties of the seafloor.

The MBES data were edited for fliers and obvious bad individual soundings (see Gardner et al., 2002 for details) and gridded into a digital terrain model (DTM) with a spatial resolution of 8 m. Individual areas were gridded into smaller DTMs at 4-m spatial resolution. Each area was analyzed with quantitative 3D visualization software that allows measurements to be made down to the pixel level (i.e., the resolution of the data).

2. Study Area

The mapped area encompasses the zone between the 40- and 150-m isobaths (Fig. 2). Existing

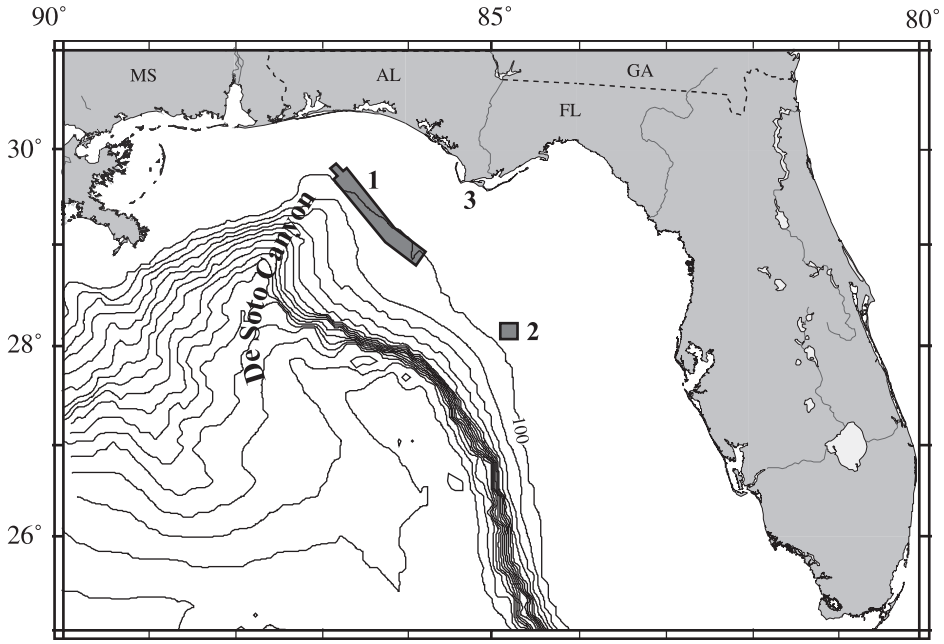

Fig. 1. Location of areas mapped with generalized 100-m contour interval. Polygon 1 extends from Destin delta and ridge to Twin Ridges delta. Polygon 2 is Steamboat Lumps. Cape San Blas of the Apalachicola River delta is labeled 3.

Table 1
Selected measurements of deltas and ridge geometries

Feature	Length (km)	Width (km)	Height (m)	Trend (degrees)	Depth range (m)	Surface gradient (degrees)	Slope (degrees)	Backscatter (dB)
Destin delta	10.540	9.860	–	–	60 to 70	0.05	2.0	−28.0 to −30.0
East Destin Ridge	18.000	0.015 to 0.100	4.0	081	56 to 66	–	17.7	−21.0 to −22.0
West Destin Ridge	27.500	0.018 to 0.650	4.0	087	56 to 66	–	6.7	−21.0 to −22.0
29-40 delta	14+	15.000	–	–	70 to 80	0.01	1.2 to 5.5	−22.0 to −30.0
A segment	2.400	<0.040	<2	010	61.5 to 62.0	–	1.8 to 5.7	−23.5
B segment	1.310	<0.050	<0.5	010	60	–	1.8	−22.5
C segment	0.278	0.100	<2	010	65	–	1.6 to 2.0	−22.0
D segment	3.200	0.040	2.0	002	65	–	2.3	−21.5
E segment	1.825	0.100	2.5	090 to 100	63	–	4.4	−22.0
F segment	3.450	0.100	2.5	080	65	–	1.4	−22.0
G segment	3.800	1.750	2.0	010	64	–	1.8	−23.0
North Coral Trees	–	–	–	–	–	–	–	−21.0
Northern segment	0.640	0.160	<4	020	86 to 95	–	7.1	−21.0
Mid-1 segment	1.100	0.270	<4	020	86 to 95	–	7.6	−21.0
Mid-2 segment	1.270	0.120 to 0.330	<4	020	86 to 95	–	5.7	−21.0
Southern segment	1.600	0.040 to 0.340	<4	130 and 005	86 to 95	–	4.1	−21.0
South Coral Trees	11.800	<0.050	–	310 to 010	83 to 88	–	–	−25.0
29-20 delta	14+	30.000		–	85	–	0.5 to 5.7	−23.5 to −25.0
Ridge 1	>12.700	0.050	1	090	52	–	3.8	−21.6 to −22.5
Ridge 2	17.950	0.020 to 0.150	<4	100	62	–	2.9 to 11.3	−21.6 to −22.5
Ridge 3	1.600	0.048	<2	135	72	–	2.6	−23.6 to −24.0
Ridge 4	1.390	0.200	<2	080 to 170	76	–	3.6	−23.6 to −24.0
Madison Swanson delta	>12.450	12.225	–	–	80 to 90	0.02	1.1 to 7.6	−22.0 to −24.0
Ridge	13.500	0.080	4 to 8	018 to 045	75 to 85	–	1.20	−20 .0
Twin Ridges delta	>9.350	12.250	–	10.0	60 to 85	0.08	1.3 to 5.7	−20.5 to 31.0
Steamboat Lumps	–	–	–	–	71 to 74	–	9.00	−28.5 to −31.0
Ridge segment	2.050	0.400	<1.0	108	72	–	1.30	−27.0 to −32.5

bathymetry of the area suggests the presence of a series of shelf-edge projections, but the projections are not well defined. Previous studies of the area have noted the shelf projections, and speculated that they probably represent relict shelf-edge deltas formed during a period of lower sea levels (Jordan, 1951; Mitchum, 1978). A study of the inner shelf in the vicinity of the Apalachicola River delta found fluvial erosion surfaces that suggest the river incised the shelf during lower stands of sea level (Donoghue, 1993) and transported sediments to the outer shelf. A recent study by McKeown et al. (2004) confirmed the delta origin of two of the shelf projections using high-resolution seismic profiling. A few accounts have been published about ridges developed on the rims of the deltas. One reports ridges identified from side-scan sonar images of the feature called Twin Ridges (Briere et al., 1999; Koenig et al., 2000; Scanlon et al., 2001), although their surveys are outside the area mapped in this study.

Several studies over the past several decades have shown that the surficial sediments in the study area consist of quartz sand (the MAFLA sand sheet) west of Cape San Blas and lime mud east of the cape (Ludwick, 1964; Doyle and Sparks, 1980; McBride and Byrnes, 1995).

The oceanic circulation in the area is dominated by periodic eddies off the anticyclonic Loop Current that flows along the continental slope and by seasonal cyclones that traverse through this part of the NE Gulf of Mexico. Although the main core of the Loop Current is west of the study area, the seafloor could have been influenced by periodic excursions of the current and its eddies (Vokovich, 1988). Surface current speeds as fast as 60 cm/s have been observed on the slope north of the De Soto

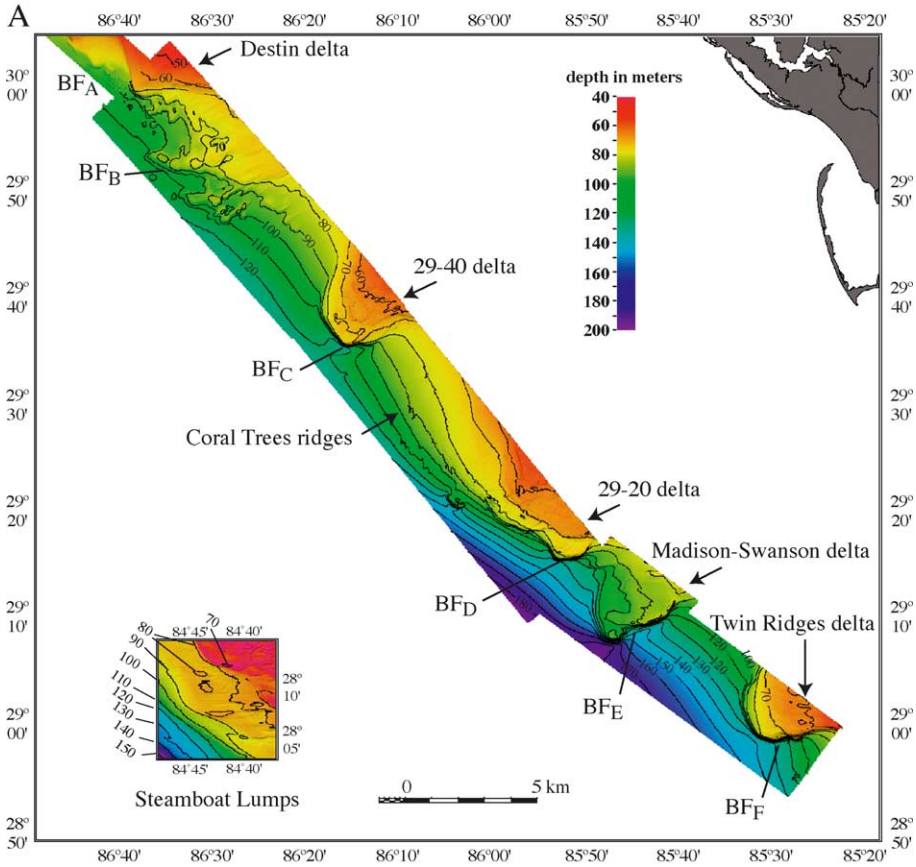

Fig. 2. (A) Overview of color-shaded relief of areas mapped. Insert map is color-shaded relief of Steamboat Lumps. Bed form fields are indicated by BF_A through BF_F. Contours in meters, illumination for bathymetry from 315°, 45° elevation. (B) Overview color acoustic backscatter draped over bathymetry of areas mapped. Insert map is color acoustic backscatter of Steamboat Lumps draped over relief Bed form fields are indicated by BF_A through BF_F.

Canyon (Molinari and Mayer, 1982). In addition, periodic hurricanes pass through the area generating cyclonic NE wind >100 kts that have the potential for significant influence on the surficial sediments in the study area.

2.1. Descriptions of shelf-edge deltas and deep-water ridges

The new MBES bathymetry shows that the outer shelf is dominated by a series of at least six SW-extending relict deltas separated by broad shelf ramps. The deltas extend out from depths shallower than the 70-m isobath. The deltas are broad, relatively flat lobes with steep (1.5° to 5°) western, northern, and southern margins that are clearly defined by the 90-m isobath (Fig. 2A). The deltas range from about 7.5 to more than 33 km wide and extend at least 3.5 km beyond the mean trend of the shelf break. The deltas are separated from one another by gently sloping (averaging about 0.3°) shelf ramps that range in width from 3.7 to 37 km and grade downslope without interruption from the <70-m depths to the 150-m isobath. All the deltas have high acoustic backscatter relative to the adjacent plains and shelf ramps (Fig. 2B). The deltas are superficially similar to features found along the outer continental shelf south of Louisiana, Mississippi, Alabama, and the Florida Panhandle (Jordan, 1951; Ballard and Uchupi, 1970; Winkler, 1982; Suter and Berryhill, 1985; Kindinger, 1988, 1989; Sydow and Roberts, 1994;

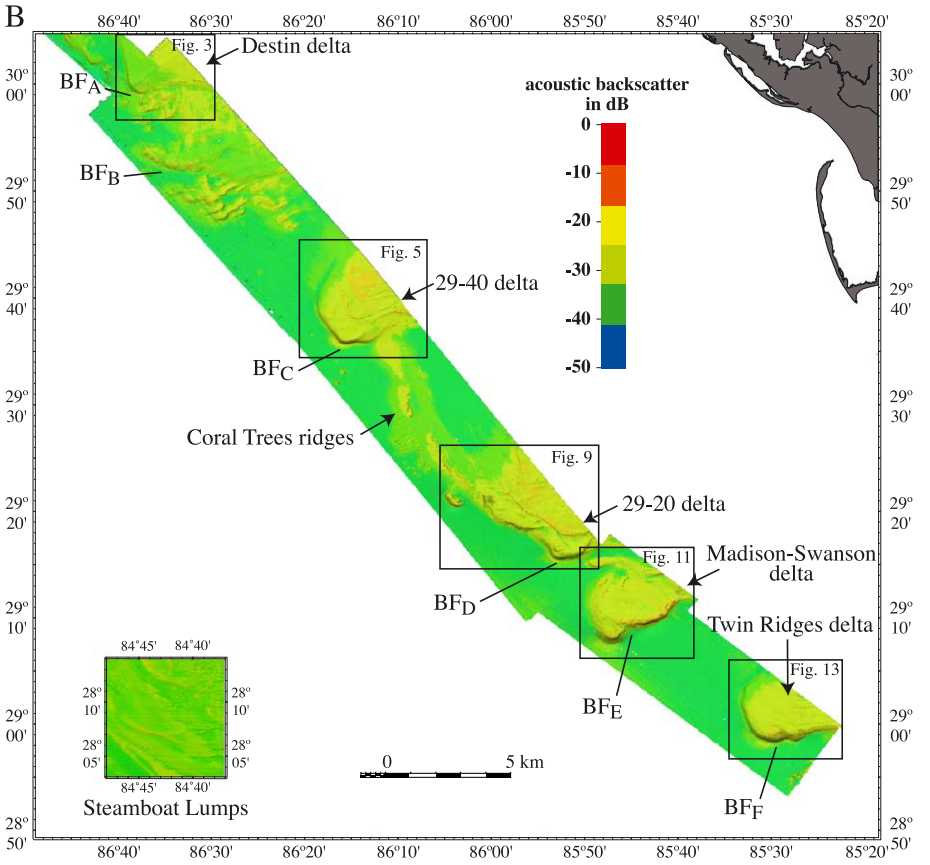

Fig. 2 (*continued*).

Morton and Suter, 1996; Sager et al., 1999; Gardner et al., 2001).

For convenience, informal names are used to refer to the shelf-edge deltas and ridges. The descriptions proceed from north to south, starting with the Destin delta, followed by the 29-40 delta, the Coral Trees ridges, the 29-20 delta, the Madison–Swanson delta, and the Twin Ridges delta, and finally Steamboat Lumps Reserve (Fig. 2A). The latter three areas derive their names from marine reserves established by the NOAA National Marine Fisheries Service, whereas the other areas are either named for their latitude or are informal names commonly used by the biological community that works in this area (K. Sulak, personnel communication, 2001).

Five of the six deltas on the NW Florida shelf have either remnants of ridges or a fully developed ridge complex on their south and SW margins in water depths of 70 to 90 m.

2.1.1. Destin delta and ridges

Destin delta is a smooth shelf extension outlined by the 60-m isobath (Fig. 2A). The surface of the delta descends from 48-m water depths on the NE to 65-m depths on the SW with a gradient of 0.05°. The SW margin of the delta drops away to the 100-m isobath with a slope of 2°, whereas the southern and western margins have slopes of about 1.4°. The surface of the delta is featureless with the exception of a series of ridges on the southern rim (Fig. 3).

Two en echelon linear ridges separated by 0.9 km are constructed on the southern margin of the delta, located at roughly 30°00′ N 86°31.5′ W (Fig. 3A, B, and C). Both ridges rise from the 65-m isobath. East

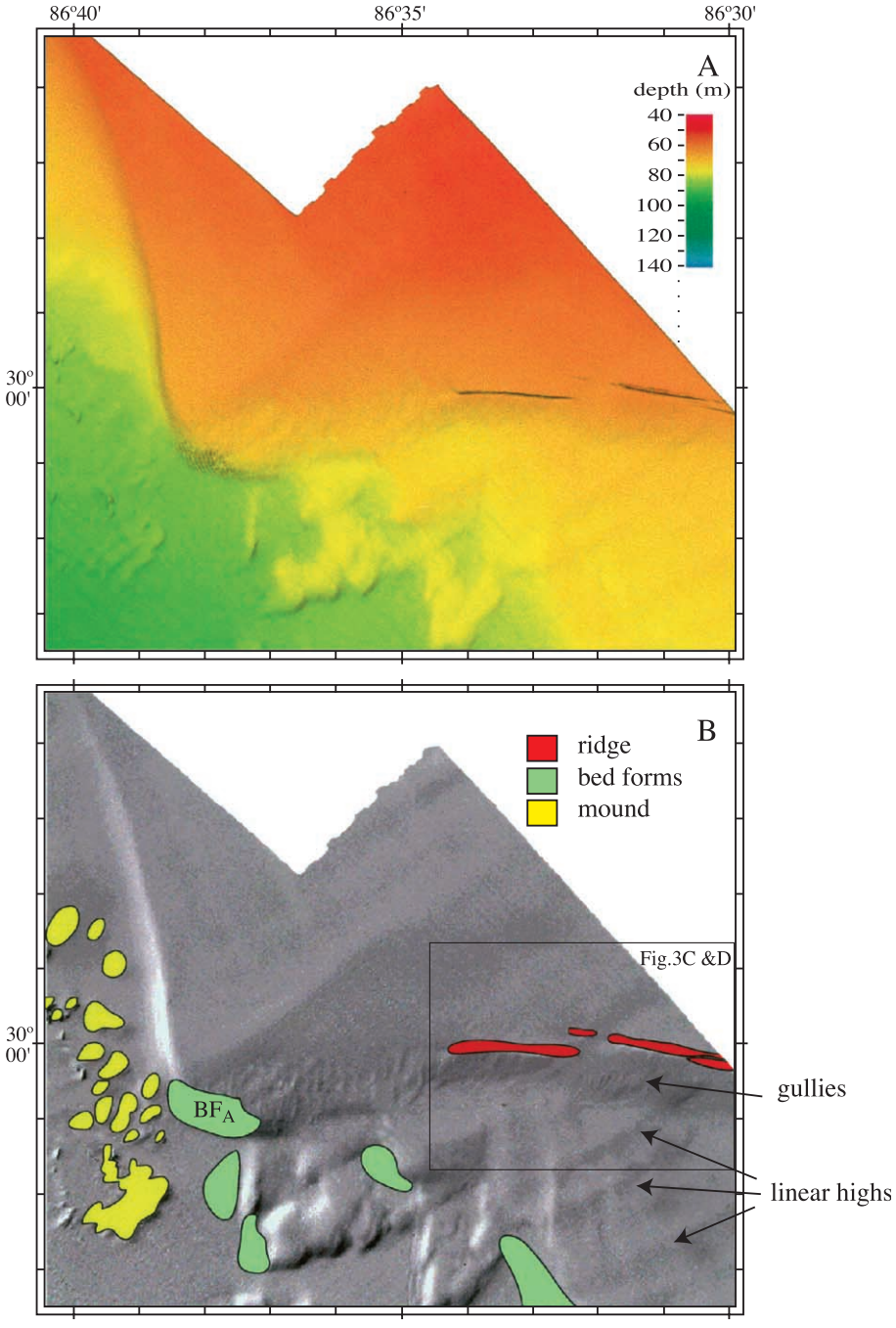

Fig. 3. (A) Color-shaded relief map view and (B) interpretation of features of Destin delta. (C) East (EDR) and west (WDR) Destin ridges shaded relief. Ridge segment labeled "c" is extension of EDR, segments "a" and "a'" are a separate ridge, and segment "b" is a third ridge trend. (D) acoustic backscatter maps at 2-m resolution. See Fig. 2 for location. Illumination for bathymetry from 315°, elevation is 45°.

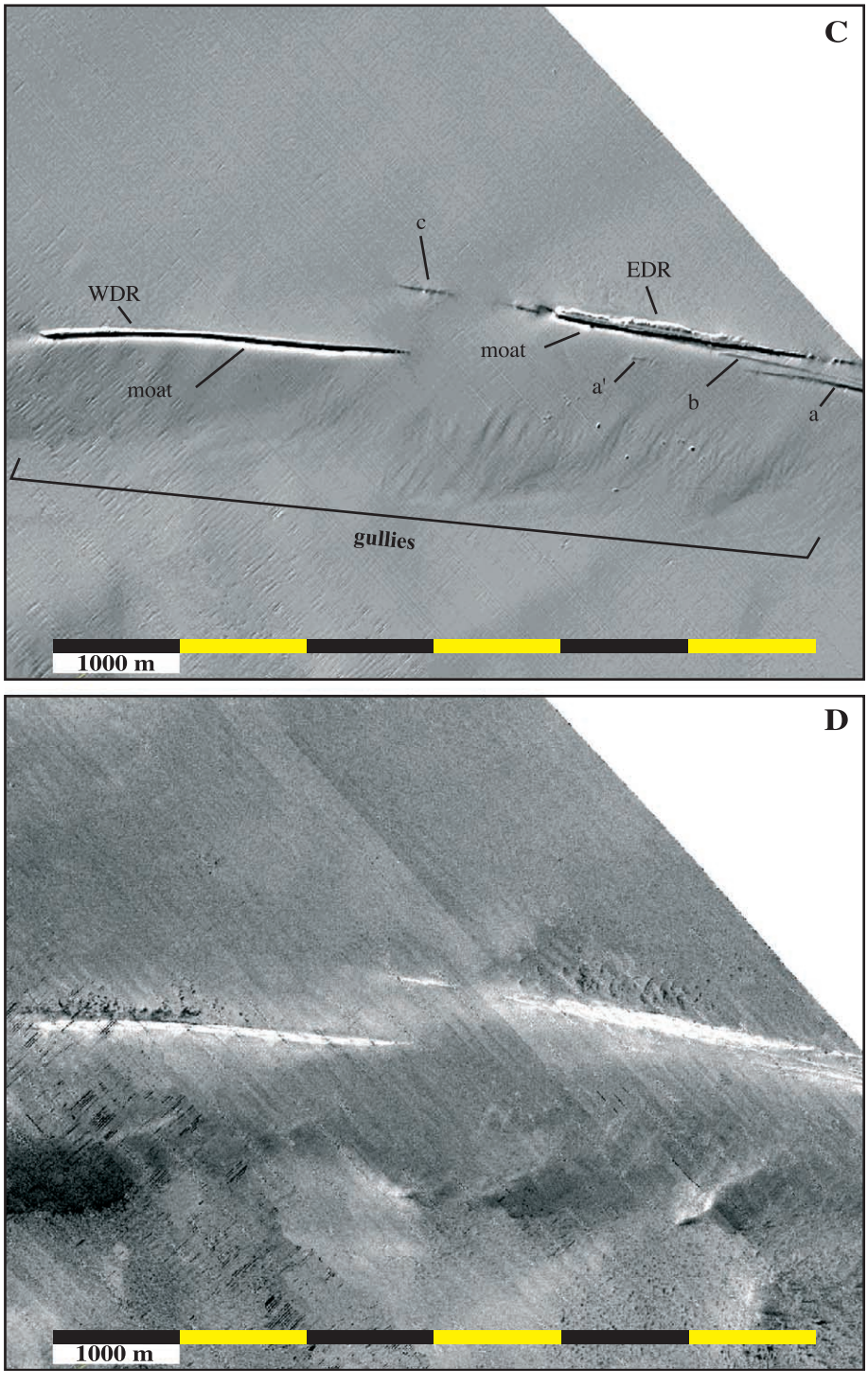

Fig. 3 (*continued*).

Destin ridge (EDR) is at least 1.8 km long and trends 081°, whereas west Destin ridge (WDR) is 2.75 km long and trends 087°. The ridges have <4 m of relief above the delta surface, and both ridges have more relief in their western section than their eastern section. The width of EDR, measured at midelevation, ranges from 15 to 100 m wide, whereas the width of WDR varies from 18 to 65 m wide. The morphologies of the two ridge segments are similar to one another, with steep (14° to 17.5°) ridge walls and narrow ridge widths. The summit of EDR is composed of three ridges, two of which parallel the ridge margins and the other somewhere between the two. The summits of the ridges are relatively rough with up to about 1 m of relief. An extension of EDR (labeled "c" in Fig. 3C) extends 900 m to the west but rises only 0.5 m above the platform surface. Two low-relief ridges trend subparallel and immediately south of EDR (labeled "a" and "b" in Fig. 3C). The ridge nearest to EDR is 20 m wide, 1300 m long, rises only 0.5 m above the seafloor, and is separated from the main ridge by 75 m. The second ridge (labeled a and a' in Fig. 3C) is 2000 m long, rises as much as 2.5 m above the seafloor, is 20 m wide, and is separated from the main ridge by 180 m. The western section of this ridge appears to be buried along a 740-m section.

An intricate gully system occurs immediately south of both ridge segments in water depths of 65 to 74 m (Fig. 3C). The gullies vary in relief from <0.2 to about 1.0 m and range from 200 to 900 m long. The length of individual gullies increases toward the west. A 20-m-wide moat, 1 to 3 m deep, occurs along the southern side of both EDR and WDR.

The acoustic backscatter of east and west Destin ridges (−21 to −22 dB) is considerably higher than the backscatter of the immediate adjacent delta surface (−28 to −30 dB; Figs. 2B and 3D; Table 1). There is a 400-m-wide halo of high backscatter that surrounds each ridge segment (Fig. 3B) and a trend of similar higher backscatter that continues to the W–SW for more than 4.6 km.

Extensive fields of bed forms are found along the southern margin of the Destin delta. A large field of well-developed bed forms occurs on the SW corner of the delta margin on a slope of 2.1° (Figs. 2A and 3B field BF_A and Fig. 4) in water depths between the 75- and 97-m isobaths. This bed form field is 3500 m long and 850 m wide with bed form crests that trend 350°. The bed forms have wavelengths of about 100 m, have wave heights that range from 2 to 4 m, and are asymmetric with the steeper side facing west (Table 2). The backscatter within the bed form field is similar to that of the adjacent featureless region.

An area of mounds occurs immediately west of the delta front in water depths of 93 to 110 m. The mounds are 150 to 600 m long, 100 to 150 m wide, and stand <2 m above the seafloor. The surfaces of the mounds appear smooth and have a high acoustic backscatter.

A 24-km-long, 16-km-wide zone of linear highs occurs immediately south of the Destin delta in water depths of 70 to 115 m (Fig. 3A and B). Twenty linear highs all trend roughly 230°. Individual highs are broad (decimeters) and are separated from one another by 1.3 to 1.8 km and rise <5 m above the immediate surrounding area. Each high has a subtly higher backscatter than the area immediately surrounding it. The highs abruptly end at 29°46.1′ N.

2.1.2. 29-40 delta and ridge complex

The 29-40 delta is located ~45 km SE of the Destin delta. This delta is 15 km wide (NW–SE) and at least 14 km long (NE–SW). The portion of the delta that was mapped has a gentle seaward slope of 0.01°. The southern margin appears to be a composite of two deltas, a partially buried delta at the 80-m isobath and the main delta at the 70-m isobath (Fig. 5). The outer margin of the main delta rises about 40 m above the outer shelf, with slopes of 1.2° on the north to 5.5° on the south. A well-developed, shelf-edge ridge complex is located in the general area of 29°40′ N 86°14′ W in water depths that range from 60 to 68 m (Fig. 5). The ridge complex encompasses >50 km^2 and is constructed along the south and west margins of the delta. The ridge is composed of seven linear to curvilinear segments (labeled *A* through *G* on Fig. 5B), aligned or abutted one to another, which range in relief from 0.5 to 5 m. The steeper face of each segment faces seaward (either west or south), with slopes that range from 1.8° to 5.7°. A topographically rough plain occurs immediately to the north or east of each ridge that is as much as 1.5 m deeper than the surrounding seafloor. A large region of relatively narrow and slightly curved ridges occurs to the west of this depression on an elevated portion of the complex. Lastly, a field of large-scale asymmetrical

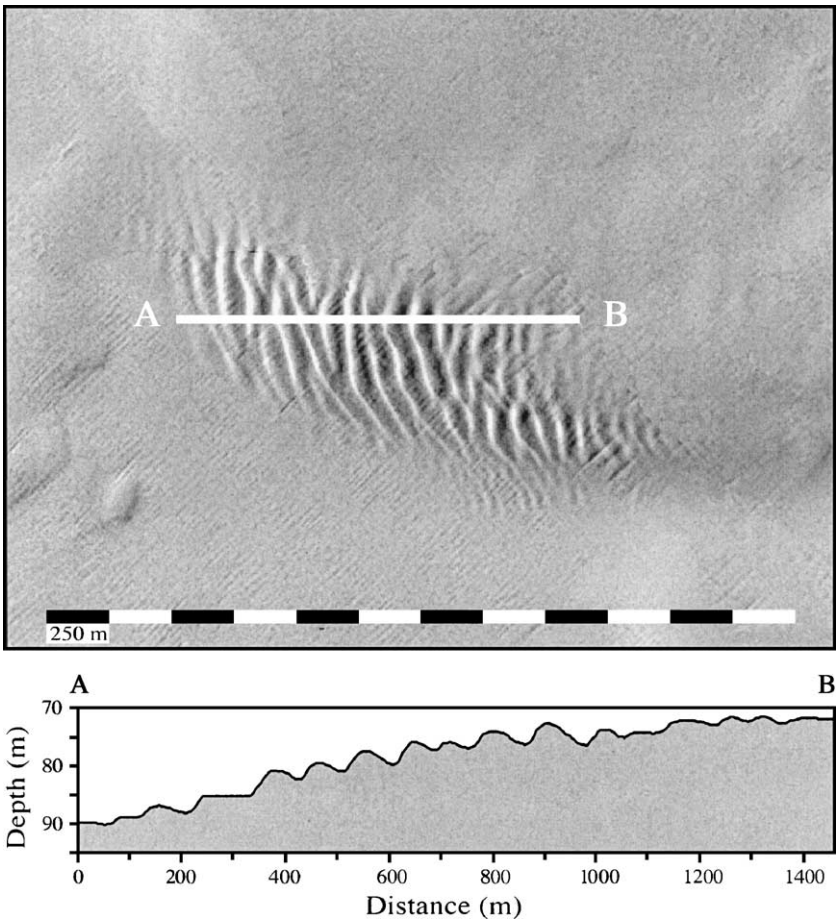

Fig. 4. Shaded-relief bathymetry map of bed form field BF_A on SW margin of the Destin platform (location BF_A in Fig. 2A). Illumination for bathymetry from 315°, elevation is 45°.

bed forms, with wavelengths of 400 to 500 m, wave heights of ~1 m, and crest trends of S–SE, covers the eastern 40% of the delta surface. Below, each ridge segment is described separately because of their unique morphologies.

Segment *A* is a slightly curved ridge that is 2.4 km long, <40 m wide, and <2 m high (Fig. 6A). The ridge rises from a base depth that varies from 61.5 to 62 m and trends roughly 010°. The southern 1000 m of segment *A* is composed of a series of low (<0.5 m)

Table 2
Bed form statistics (all values in meters, except area is km^2; symmetry of bed form profile is asy: asymmetric, sym: symmetric)

Bed form field	Wave length (m)	Length σ	Wave height (m)	Height σ	Water depth (m)	Symmetry
Bfa	85.5	17.0	0.8	0.3	82 to 97	asy
BFb	46.8	8.4	0.4	0.3	99 to 108	asy
BFc	70.9	14.9	0.7	0.3	78 to 122	asy
BFd	85.1	18.9	1.1	0.4	85 to 97	asy
Bfe	53.7	6.9	0.8	0.2	98 to 103	asy
BFf	101.3	25.3	1.4	0.7	80 to 115	asy

Refer to Fig. 2A,B for location of bed form fields.

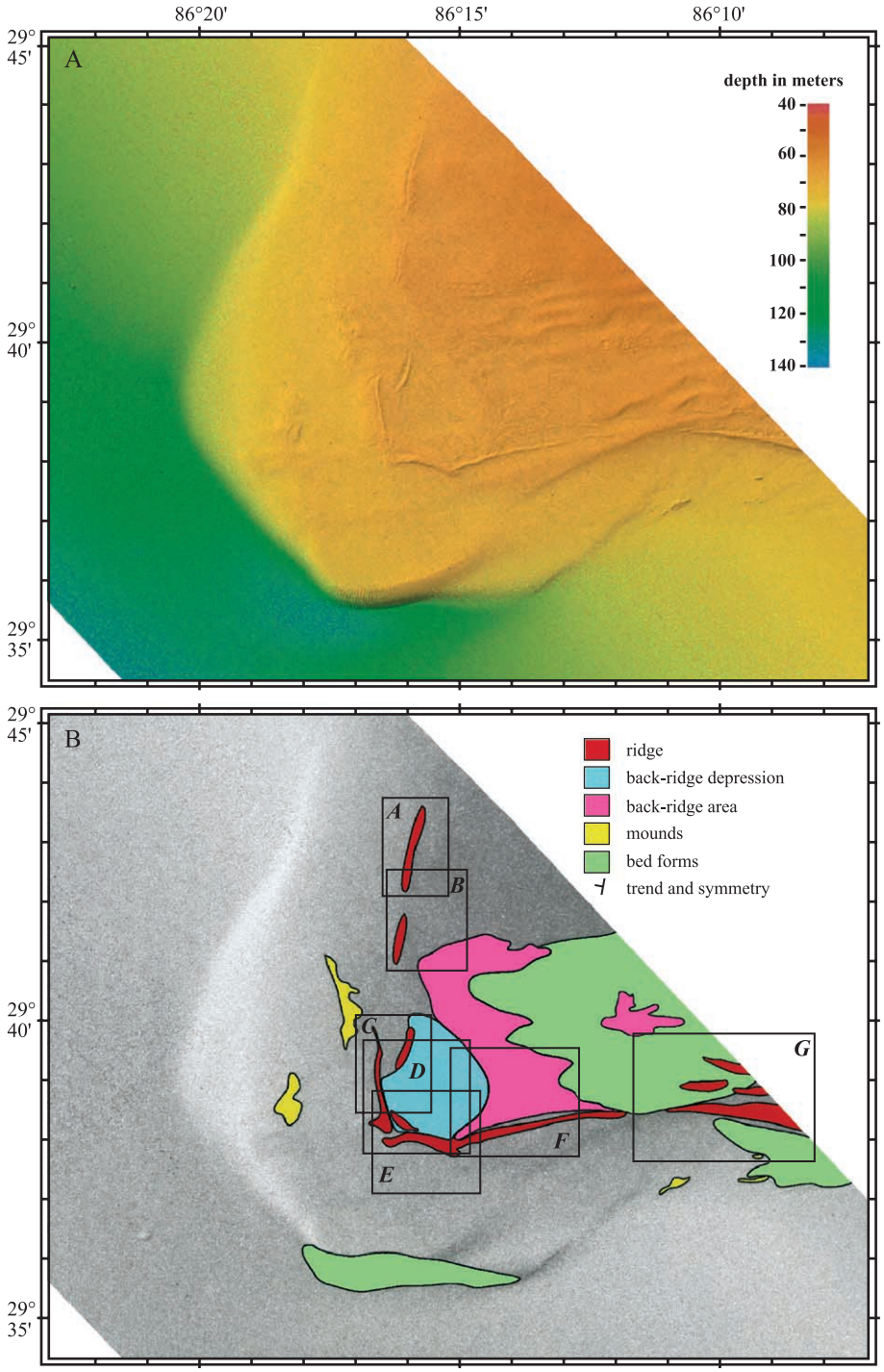

Fig. 5. (A) Color-shaded relief map view and (B) interpretation of features of 29-40 delta. See Fig. 2 for location. Polygons are locations for Fig. 6. Illumination for bathymetry from 315°, elevation is 45°.

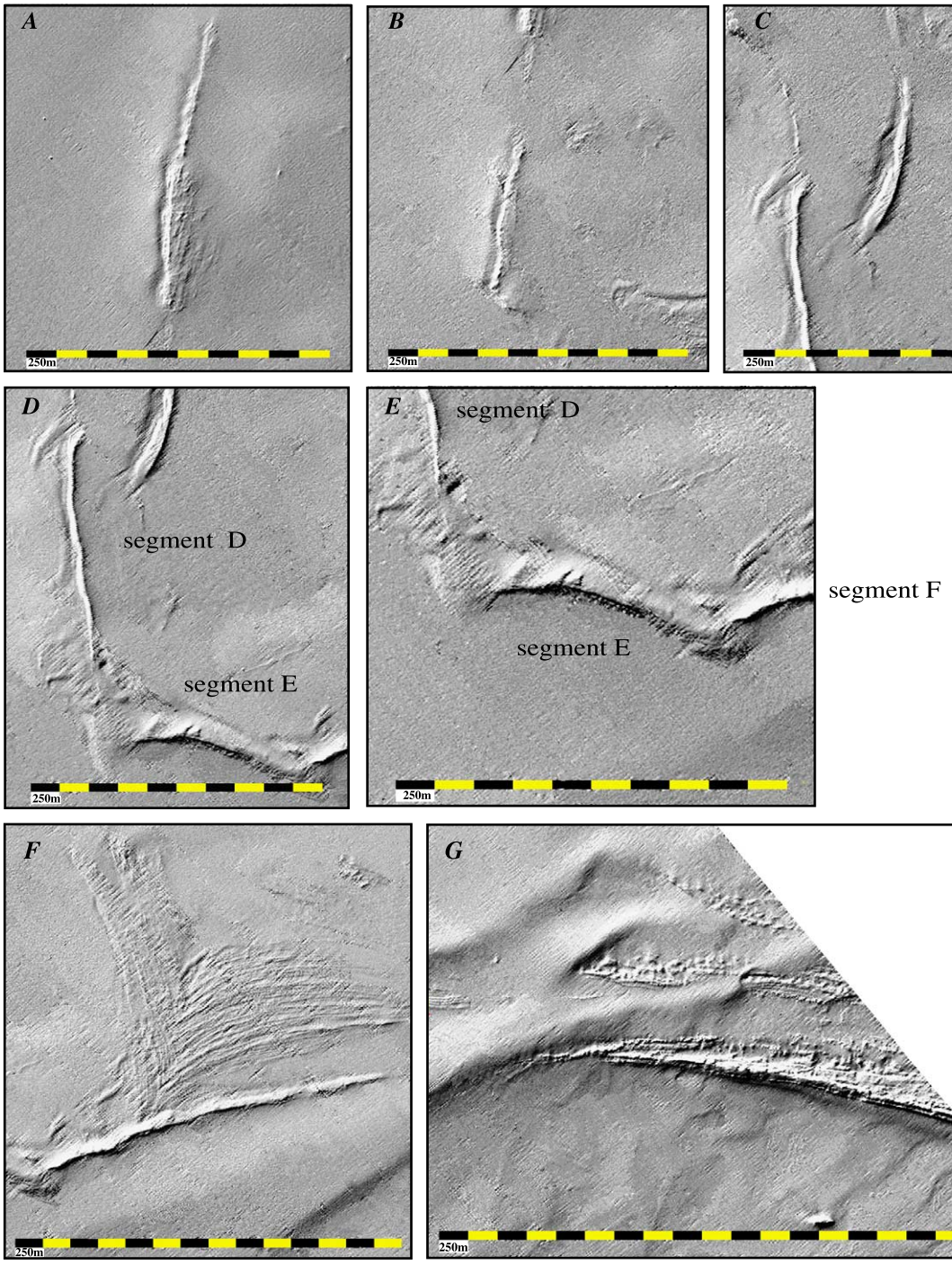

Fig. 6. Shaded-relief bathymetry maps of 29-40 ridge segments: (A) segment A; (B) segment B; (C) segments C and north half of segment D; (D) southern half of segment C, segment D, and segment E; (E) south half of segment D, segment E, and western portion of segment F; (F) segment F and beach–ridge ridges; (G) segment G showing partial burial by sediment dunes. North orientated, no vertical exaggeration. Illumination for bathymetry from 315°, elevation is 45°.

ridges. This ridge does not have an appreciable acoustic backscatter signature. A 0.5-m-deep, <60-m-wide moat parallels the west side of the ridge. The moat abruptly ends where the ridge terminates.

Segment *B* is a 1310-m-long, straight section of ridge (Fig. 6B) separated from, but aligned with, segment *A* by an 884-m gap. Segment *B* trends 010°, has <0.5 m of relief, and is everywhere <50 m wide. This ridge has no acoustic backscatter signature. A moat similar to the one that parallels segment *A* is found beside segment *B* along its west side. The moat is about 50 m wide and <1 m deep.

Segment *C* is a 278-m-long, curved ridge separated by 2170 m from the southern end of segment *B* and set to the east by 600 m (Fig. 6C). Segment *C* rises from the 65-m isobath, is about 100 m wide, and <2 m high, and also trends roughly 010°. A 2-m-deep moat up to 100 m wide parallels the west side of this segment. The ridge has a higher acoustic backscatter values than the immediate area surrounding the segment.

Segment *D* is a curved 3200-m-long ridge that rises up to 2 m above the 65-m isobath (Fig. 6D). This segment is about 40 m wide throughout its length except on the ends. The northern end of segment *D* is not aligned with the southern end of segment *C*; it is en echelon with it with an overlap of 1310 m and set to the west by 600 to 1000 m. This segment has a trend of 178°. The ridge has a distinctly higher acoustic backscatter than does the surrounding seafloor. A moat <0.5 m deep and as much as 30 m wide parallels this segment immediately west of the ridge.

Segment *E* (Fig. 6E) is a curved ridge that trends 090° to 100°. The ridge is 1825 m long, about 100 m wide, and rises up to 2.5 m above the 63-m isobath. The junction of segments *D* and *E* is a broad complex area about 500 m wide, 1000 m long, and 0.5 m shallower than the adjacent seafloor. The ridge has higher acoustic backscatter compared to values of the immediately adjacent seafloor. A short section of raised seafloor, possibly a ridge, is found immediately to the north of segment *E* and immediately east of segment D. The raised area is about 800 m long, trends about 310°, but rises only 0.5 m above the surrounding seafloor. It is unclear whether this short section actually joins either the *D* or *E* segments. No moat was found adjacent to segment *D*.

Segment *F* is a slightly curved, 3450-m-long, 100-m-wide ridge that rises as much as 2.5 m above the 65-m isobath (Fig. 6F). This segment trends 080°, and its western end abuts segment *E* at a 45° angle. The ridge has higher backscatter values than does the adjacent seafloor to the south. The area immediately north of segment *F* is a complex region with two curved orthogonal sets of ridges. The ridges are only 0.25 m high, 10 to 20 m wide, and as much as 2000 m long. The ridges are the surface of an area of the platform that stands 1.5 m shallower than the surrounding regions. No moat is evident adjacent to segment *F*.

The *G* segment, which is morphologically very different, is composed of at least five ridges amalgamated into a structure (Fig. 6G). This segment is slightly curved, 3800 m long, and more than 1750 m wide. This segment is partially buried by the large bed forms described above. The rough topography of this segment rises up to 2 m above the 64-m isobath. The segment *G* ridge has a higher backscatter than the immediate seafloor. No moat parallels this ridge segment.

2.1.3. Coral Trees ridges

An en echelon series of four ridges (Figs. 2A, 7, and 8) occurs approximately 13.8 km south of the 29-40 platform in water depths of 86 to 95 m. The four ridges collectively are called north Coral Trees ridges. These ridges are not developed on a shelf platform but rather are constructed on a broad shelf ramp. The four segments of north Coral Trees ridges morphologically resemble each other; they only differ in their lengths and shape (Fig. 8D). The northern-most ridge segment is 640 m long and 160 m wide; the next segment in line is 1100 m long and 270 m wide; the third segment is 1270 m long and ranges in width from 120 to 330 m wide; and the southern segment is 1600 m long, has a pronounced change in trend 1060 m from its northern end, and ranges from 40 to 340 m wide. The northern three segments have similar trends of 020°, whereas the southern segment has a trend of 355° for its northern section and a trend of 230° for its southern section (Fig. 8D). Each of the north Coral Trees ridges has as much as 4 m of relief, and in addition, each has numerous circular pinnacles with diameters as large as 20 m and heights of 2 to 3 m above the main ridge structure. These

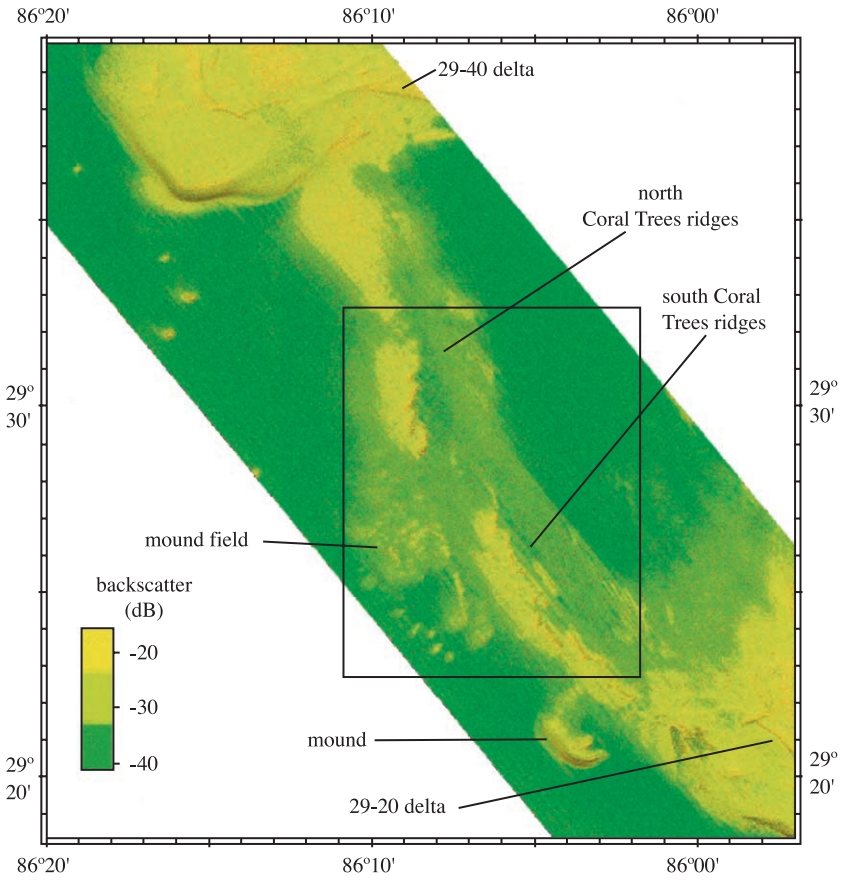

Fig. 7. Acoustic backscatter map draped over bathymetry of Coral Trees ridges. Black polygon shows locations for Fig. 8.

pinnacles resemble pinnacle reefs described in similar water depths on the outer continental shelf south of Mississippi, Alabama, and Texas (Gardner et al., 1998, 2001). The three northernmost of the north Coral Trees ridges have a moat adjacent to the west side of the structure, generally about 20 m wide and up to 1 m deep.

Acoustic backscatter of the ridges is higher than the area immediately to the east of the ridges. However, the area immediately west of the ridges have intermediate backscatter values (Fig. 8B and C), suggesting very different materials, different bed roughness, or differences in shallow subsurface inhomogenieties on either side of the ridges. Profiles across each of the ridges show that sediment has banked as much as 3 m deep behind the ridges (Fig. 8E). The north Coral Trees ridges are part of a band of high backscatter that extends from the southern margin of the 29-40 platform to the 29-20 platform (discussed below) confined to water depths between 80 and 100 m (Fig. 7).

A band of at least eight ridges, collectively called south Coral Trees ridges, is found about 4 km south of the north Coral Trees ridges between water depths of 83 and 88 m (Fig. 2A). These ridges have morphologies similar to the north Coral Trees ridges. South Coral Trees ridges occur along the eastern margin of the high-backscatter zone and join with the NW margin of the 29-20 delta (Fig. 7). The general trend of the main body of the south Coral Trees ridges is 310°, but the trends of individual ridges range from 310° to 010°. The summit areas of the ridges are composed of numerous pinnacles similar to those found on the Coral Trees ridges.

Areas of broad smooth mounds are found SW and W of both the Coral Trees ridges and southern Coral

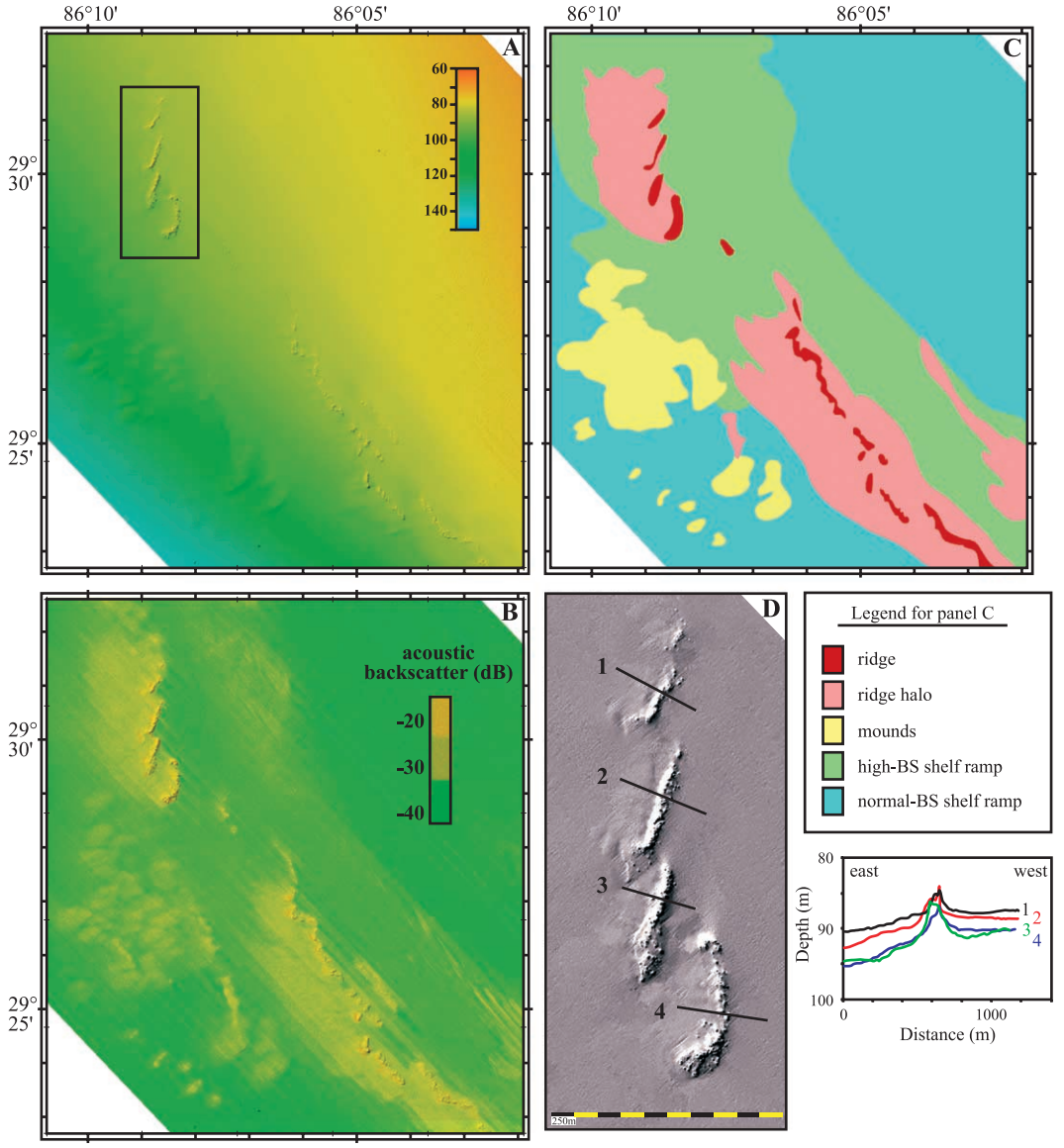

Fig. 8. (A) Color-shaded relief map view of Coral Trees ridges. Black polygon is location of Fig. 8D. (B) Color acoustic backscatter draped over bathymetry. (C) Interpretation of features. (D) Gray-scale-shaded relief map of northern Coral Trees ridges with profiles. Illumination for bathymetry from 315°, elevation is 45°. See Fig. 7 for location.

Trees ridges (Fig. 8C). The mounds range up to 850 m long and 450 m wide and have as much as 5 m of relief. All of the mounds are oriented with their long axis trending SW, essentially down the regional bathymetric gradient. The area encompassed by the mounds is about 13 km^2 and lies between the 98- and 119-m isobaths.

A large, isolated, somewhat kidney-shaped, smooth mound occurs 3.5 km SW of the southernmost of the south Coral Trees ridges at about 29°21′ N 86°04′ W between the 120- and 100-m isobaths (Fig. 7). The mound is 4 km long, about 700 m wide, and 20 m high. An arm located about 2000 m south of the northern end of the mound

extends 800 m upslope, perpendicular to the main trend of the mound.

2.1.4. 29-20 delta and ridge complex

The 29-20 delta is located about 18.5 km SW of the 29-40 delta (Figs. 2 and 9). The feature is a large composite platform with at least two partially buried lobes and a main large lobe that spans almost the entire distance between the 29-40 delta to the northwest and the Madison–Swanson delta to the southeast. The partially buried lobes are found at the 75- and 80-m isobaths. The top of the 29-20 delta is 30 km wide (NW–SE) and extends at least 14 km to the SW. The main delta rises abruptly (4.6°) on the SW side between the 130- and 85-m isobaths. The south side has a steeper gradient (5.7°), whereas the northwestern margin of the delta has slopes of only 0.5°. The 29-20 ridge complex is constructed on the SW part of the delta and is composed of a series of ridge complexes built upon older, some partially buried, ridge complexes. The deepest ridge (labeled "4" in Fig. 9) is found along the 76-m isobath, but only a small section is exposed. The section is 1390 m long, has <2 m of relief, and has a 200-m-wide, 1.5-m-deep moat adjacent to its north side.

The next shallower ridge is exposed as two sections along the 70-m isobath that are separated by 13 km along a NW–SE trend (labeled "3" in Fig. 9). The two sections morphologically resemble one another, but they appear not to be connected. The southern section is 1600 m long with an 85° bend roughly in the middle of its length (Fig. 10A). A 50-m-wide, 2-to 4-m-deep moat has formed immediately west of the north–south limb of the ridge. The northern section is 1760 m long and trends NW–SE and has no moat.

A large ridge complex is found along the 65-m isobath (labeled "2" in Fig. 9), similar to the 29-40 ridge complex, although without a back-ridge depression. The ridge front is composed of four straight to slightly curved segments, totaling 17.95 km in length and varying in width from 20 to 150 m. The ridge front has from 2 to 4 m of relief with outer slopes that range from 2.9° to 11.3°. A 1-m-deep, 20-m-wide moat is found immediately seaward of the SW-facing sections of the ridge front. A 440-m-wide pass is located along the SW-facing portion of the ridge (Fig. 10B).

The shallowest ridge front (labeled "1" in Fig. 9B) occurs along the 55-m isobath in the northern third of the area occupied by the older ridge complex. Together, the two youngest ridge complexes encompass more than 80 km^2, whereas the youngest complex alone covers at least 24 km^2. The ridge fronts have from 4 to 6 m of relief along their seaward sides, and the back-ridge areas are consistently 4 to 5 m shallower. Although most of the 70-m ridge complex has been buried by sediment, the northern portion of the ridge is exposed enough to demonstrate a pattern of ridges perpendicular to the main ridge front (Fig. 10D, E). Most of the back-ridge area of the 55-m ridge complex is exposed and shows an intricate pattern of ridges and high acoustic backscatter. In addition, many of the back-ridge features resembles hard grounds that are common on the outer continental shelf off Alabama and Mississippi (Gardner et al., 2001; Fig. 10C).

All of the ridges have relatively high acoustic backscatter. The shallower ridges have higher backscatter values than the deeper ones. The areas immediately adjacent to the ridges have lower backscatter than the ridges (Fig. 10E).

Fields of bed forms are found along the south and SW margins of the 29-20 delta (field BF_D in Fig. 2A). The major bed form fields are found in a water-depth zone of 75 to 130 m. These bed forms have wave heights of 2 to 4 m and wavelengths that range from 60 to 140 m. The bed forms become strongly asymmetric with increased water depth. The bed form crests are perpendicular to the contours, and their steepest sides always face W–NW. The bed form crests of fields "X" and "Y" (Fig. 9) are linear, and individual crests can be traced for more than 1500 m. The bed forms of field "Z" have short, curved and kinked crests showing convincing evidence of partial burial by a thin blanket of sediment (Fig. 10F).

A large field of pockmarks occurs in water depths of 115 to 120 m (Fig. 9). The field is 5275 m long and 925 m wide, covering almost 5 km^2 with a pockmark density of 88 per km^2. The pockmarks range from 10 to 20 m in diameter and are 1.0 to 1.5 m deep.

2.1.5. Madison–Swanson delta and ridge

The Madison–Swanson delta is located immediately SE of the 29-20 delta (Fig. 2). McKeown et al. (2004) presented high-resolution, seismic-reflection

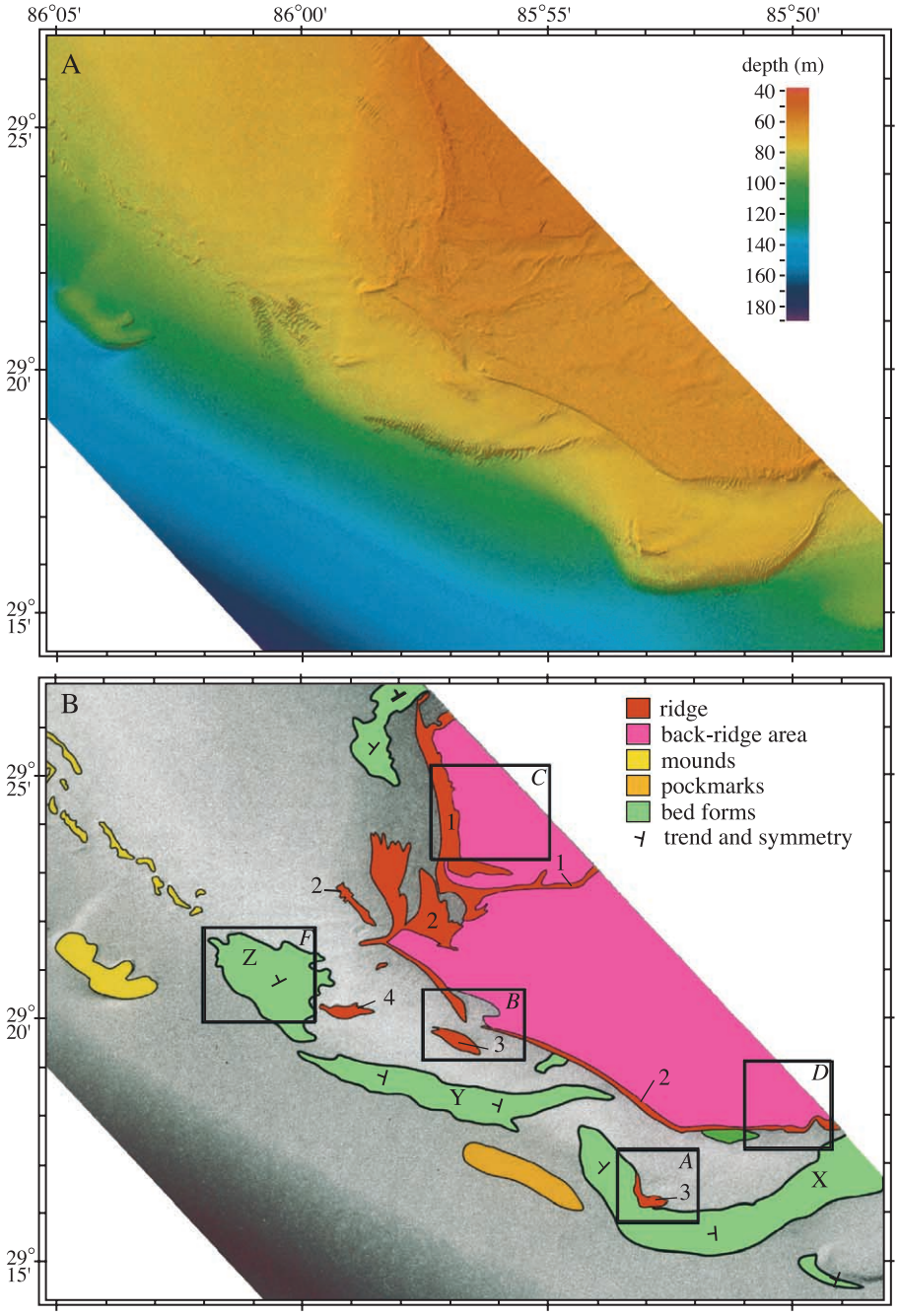

Fig. 9. (A) Color-shaded relief map and (B) interpretation of features of 29-20 delta. See Fig. 2 for location. Polygons "a" through "f" are locations for Fig. 10. Numbers 1 through 4 identify ridges of different age (see text for details). Illumination for bathymetry from 315°, elevation is 45°.

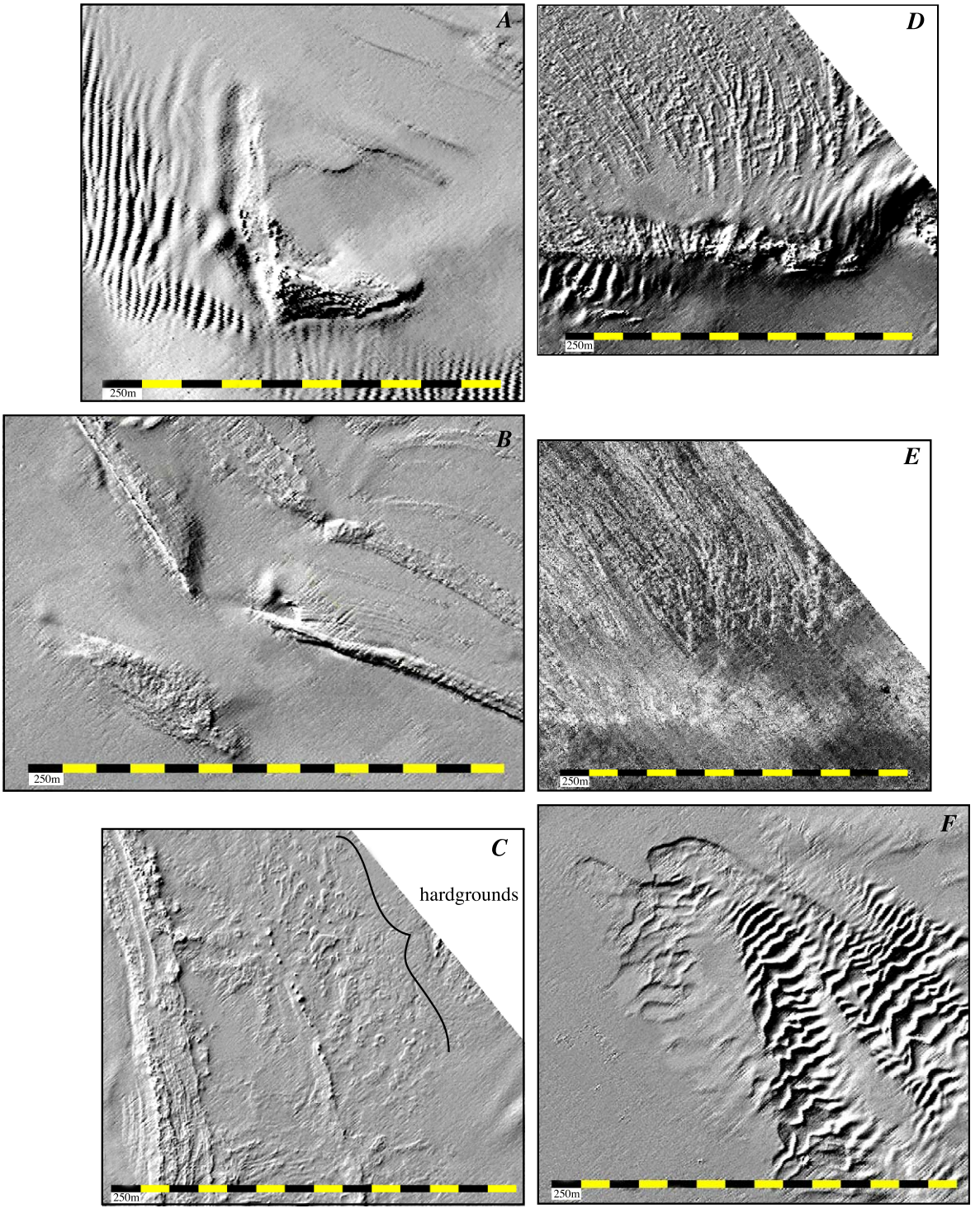

Fig. 10. Shaded-relief (A, B, C, D, and F) views of segments of 29-20 ridge. Illumination for bathymetry from 315°, elevation is 45°. Acoustic backscatter (E) is of area shown in (D). See Fig. 9 for locations and text for discussion.

data that show the foreset clinoforms of this delta. The surface of the Madison–Swanson delta is in 80- to 90-m water depths and gently sloping at 0.02° to the southwest (Fig. 11). The south and western margins of the delta rise about 40 m above the outer shelf with slopes of 7.6° on its southern margin, 6.3° on its SW margin, and 1.1° on its western margin. The main ridge front has formed an almost continuous 13.5-km-long rim along the southern edge of the platform in water depths that range from 75 m on the east to 85 m on the west. The curvilinear ridge front rises 4 to 8 m high, is highest in the eastern section, and is as much as 80 m wide. The ridge front bifurcates on its eastern end with one ridge segment at the 85-m isobath and another at the 80-m isobath, with as much as 720 m of separation (Fig. 12A). The main ridge has a rough microtopography with as much as 3 m of relief. An extensive back-ridge area covers at least 70 km^2. A moat up to 1 m deep and 50 to 100 m wide parallels the ridge front on its landward (north) side (Fig. 12A). A large, shallow depression is located immediately behind (shoreward) the western third of the ridge front. The depression is 5.37 km long and 2.59 km wide and is about 2 m deeper than the adjacent relatively featureless delta surface.

Another area of ridge is found at the 80-m isobath in the NE part of the delta. Only a segment of this ridge was mapped, but it may be a continuation of a large area of ridge found to the SE at the 72-m isobath. This ridge has a 160-m-wide, flat-topped summit at the 72-m isobath. This segment is at least 2.7 km long. The ridge area to the SE is a broad area of ridges seen in the background in Fig. 12A.

A third area of ridges is found along the 90- to 95-m isobaths in the NW part of the delta. These ridges are short (350 to 400 m long) en echelon ridges that rise less than 2 m above the delta surface. These ridges appear to be partially buried by sediment, and only short pinnacles project above the sediment blanket.

Acoustic backscatter of the Madison–Swanson delta mimics that of the other delta described above (Fig. 2B). Backscatter values of the ridge complexes are typically higher than the surrounding platform surface, and the backscatter of the platform is typically higher than the deeper outer shelf. Two areas of high backscatter occur on the outer shelf adjacent to the Madison–Swanson delta; one area extending SW beyond the SW corner of the delta and the other just beyond the west-facing margin of the delta. These two areas have higher backscatter values than the immediate outer shelf.

Several areas of mounds occur on the Madison–Swanson delta (Fig. 11). The mounds resemble those described in the Coral Trees ridges area. The mounds occur as groups of individual mounds, and some occur with a linear trend (Fig. 12B). The mounds are found along the 102-m isobath and are typically elliptical in plan view with major axes up to 650 m in length and minor axes up to 400 m in length. The mounds have up to 4 m of relief and invariably have a 20-m-wide, 1-m-deep moat on their NW side.

Several large fields of bed forms are found around the southern and western margins of the delta and immediately seaward on the outer shelf (Fig. 11). The bed forms on the delta occur in water depths of 84 to 87 m, whereas those of the outer shelf occur in water depths of 100 to 120 m. The bed forms are all fairly uniform in size, ranging in wavelength from 40 to 70 m with wave heights from 0.5 to 2 m. The bed form fields can be divided into those seaward of the ridges on the flanks of the delta and those landward of the ridges on the surface of the delta. The bed forms in the shallower water generally have smaller wave heights than those in deeper water. The bed forms are all asymmetric, with the degree of asymmetry increasing with water depth. The steeper sides of the bed forms along the southern margin face west, but face N–NW along the western margin, and those on the delta surface face N–NW.

2.1.6. Twin Ridges delta

The Twin Ridges delta is located 17.6 km southeast of the Madison–Swanson delta and is found in water depths ranging from 60 m on the SE to 85 m on the SW (Fig. 2). The western and southern portions of the delta have been described from high-resolution seismic-reflection profiles (McKeown et al., 2004), side-scan sonar imagery, high-resolution seismic profiles, and surficial-sediment sampling (Briere et al., 1999; Scanlon et al., 2001). Briere et al. (1999) documented the existence of two parallel ridges, called “rocky ledges” by the authors, which are located immediately south of the SE corner of the mapped area. Briere et al. (1999) states that the

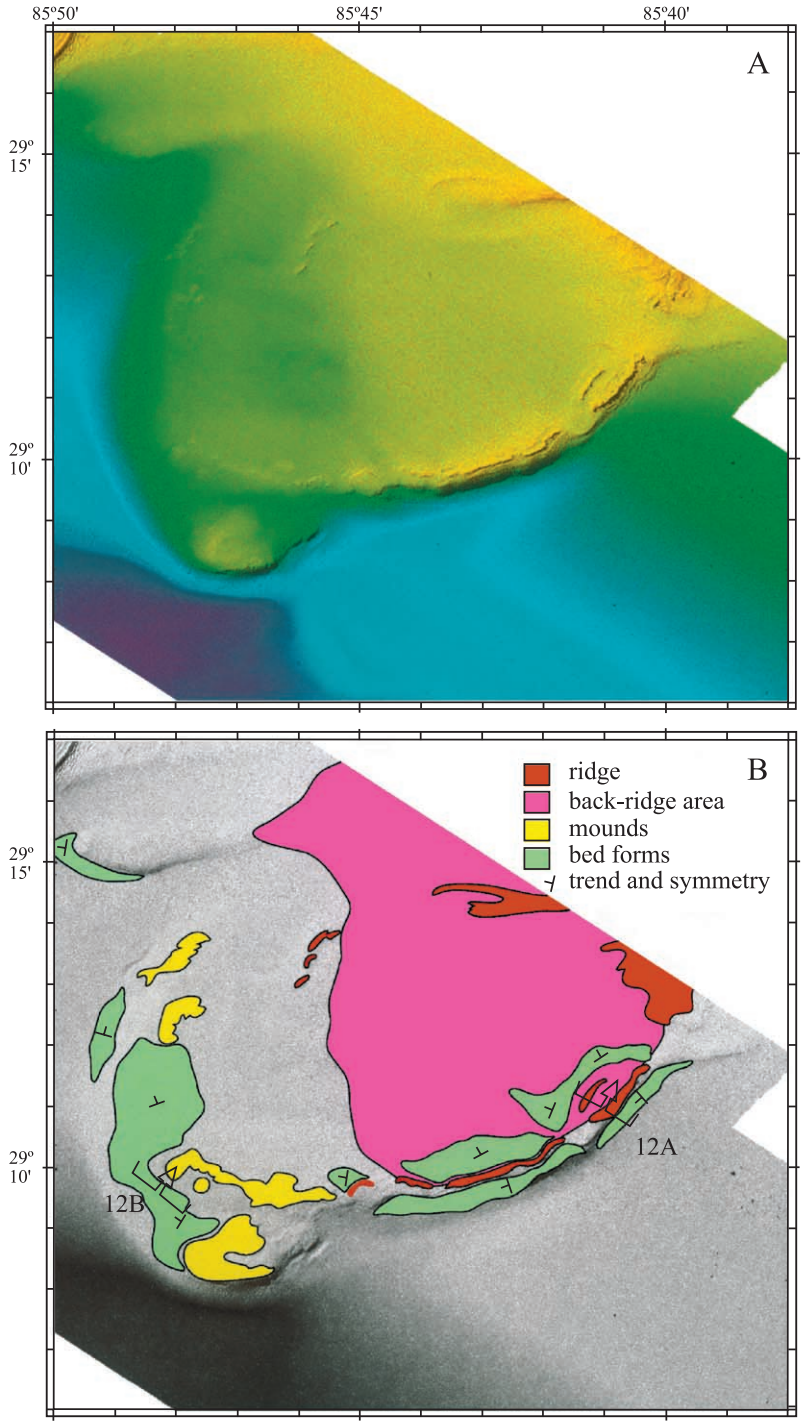

Fig. 11. (A) Color-shaded relief map view and (B) interpretation of features of Madison–Swanson delta. See Fig. 2 for location. Open arrows point in view direction for Fig. 12A and B. See text for discussion.

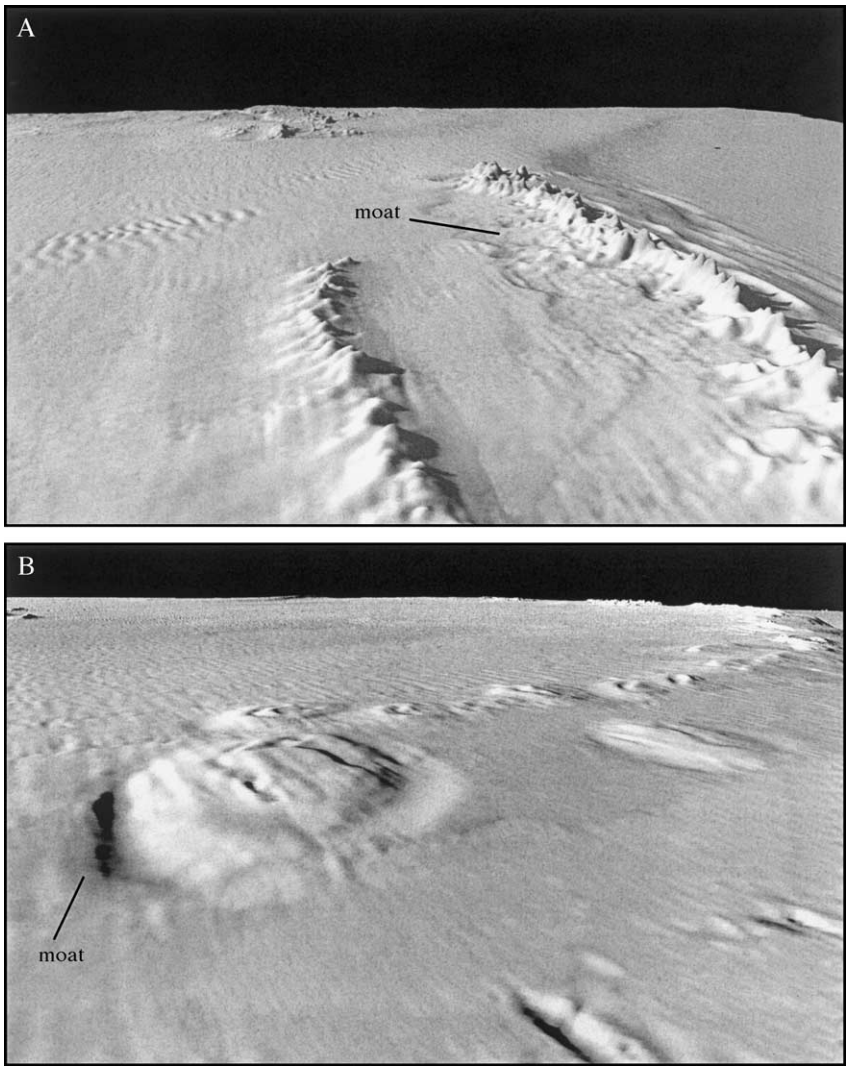

Fig. 12. (A) Oblique view of SE Madison–Swanson delta showing the rough nature of the ridge crests and 1-m-deep moat on north side of southern ridge. Distance across bottom 900 m; vertical exaggeration 6×. (B) Oblique view of SW Madison–Swanson delta showing elliptical mounds. Distance across bottom 660 m; vertical exaggeration 6×. See Fig. 11 for locations.

southern and western areas of the platform are blanketed by a gravelly to medium to coarse quartz sand, whereas the areas of the platform margin in water depths deeper than 90 m are covered by a silty sand with minor gravel and clay. In addition, they identified areas of bed forms along the periphery of the delta.

The surface of the Twin Ridges delta has a gentle gradient of 0.08° toward the south. The surface of the delta is relatively smooth, with the exception of a rim followed by a depression along its southern margin (Fig. 13). The delta-top depression is set back from the rim by 100 to 200 m and varies in relief from 1 to 3 m. The SW margin of the delta is much steeper (5.0° to 5.7°) than the other margins (1.3° to 1.7°; Fig. 13). The surface of the Twin Ridges delta has higher acoustic backscatter values along the SW rim of the platform than over the rest of the feature. The backscatter values are generally higher along the southern part of the platform compared to the northern

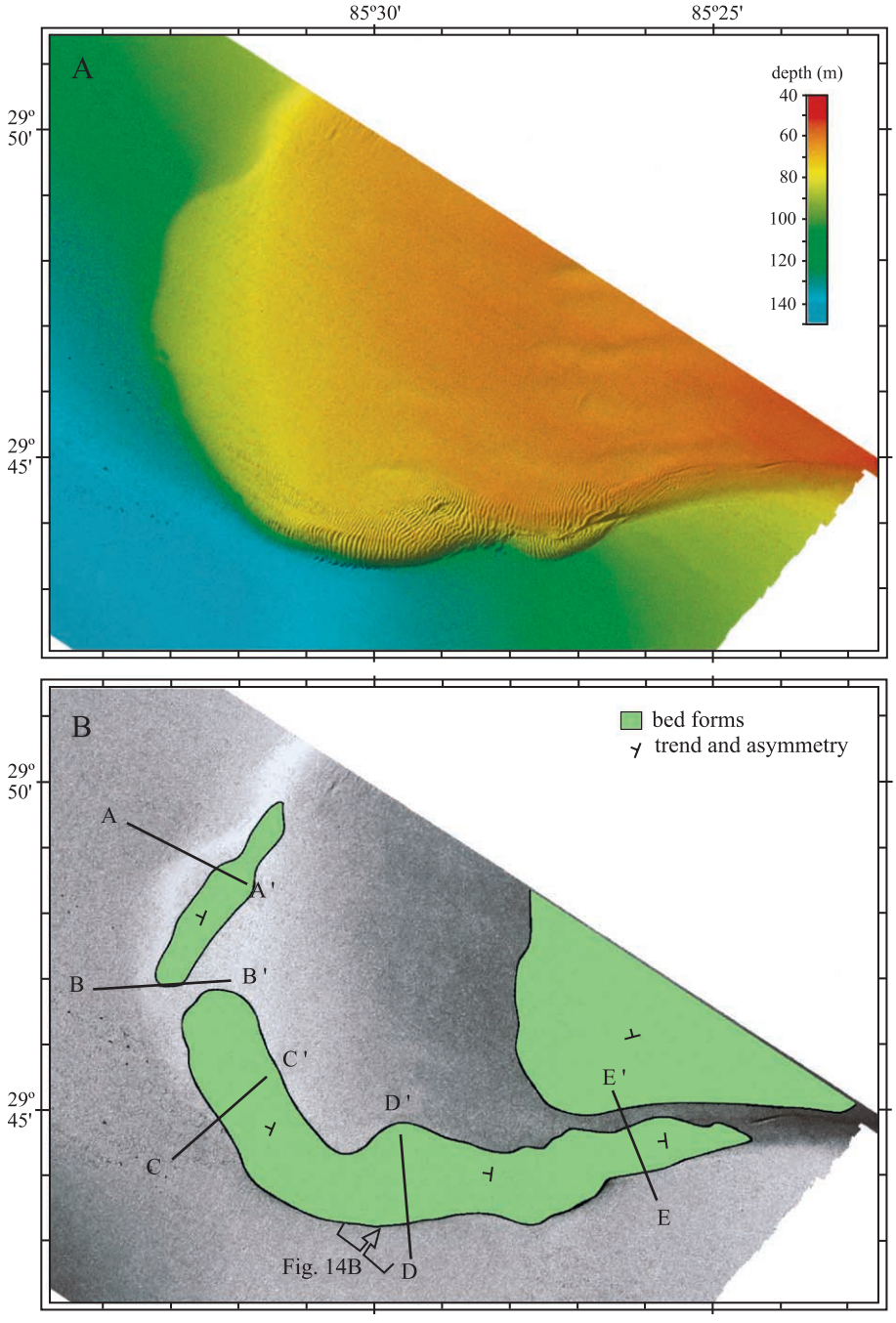

Fig. 13. (A) Color-shade relief map view and (B) interpretation of features of Twin Ridges delta. See Fig. 2 for location. Open arrows point in view direction for Fig. 14B. Illumination for bathymetry from 315°, elevation is 45°. Lines are locations of profiles in Fig. 14A.

and western portions. A distinctive area of higher backscatter occurs off the SW margin of the delta on the deeper seafloor.

A large field of bed forms is present along the south and SW margin of the delta (Fig. 14). This is the bed form field identified by Briere et al. (1999). The

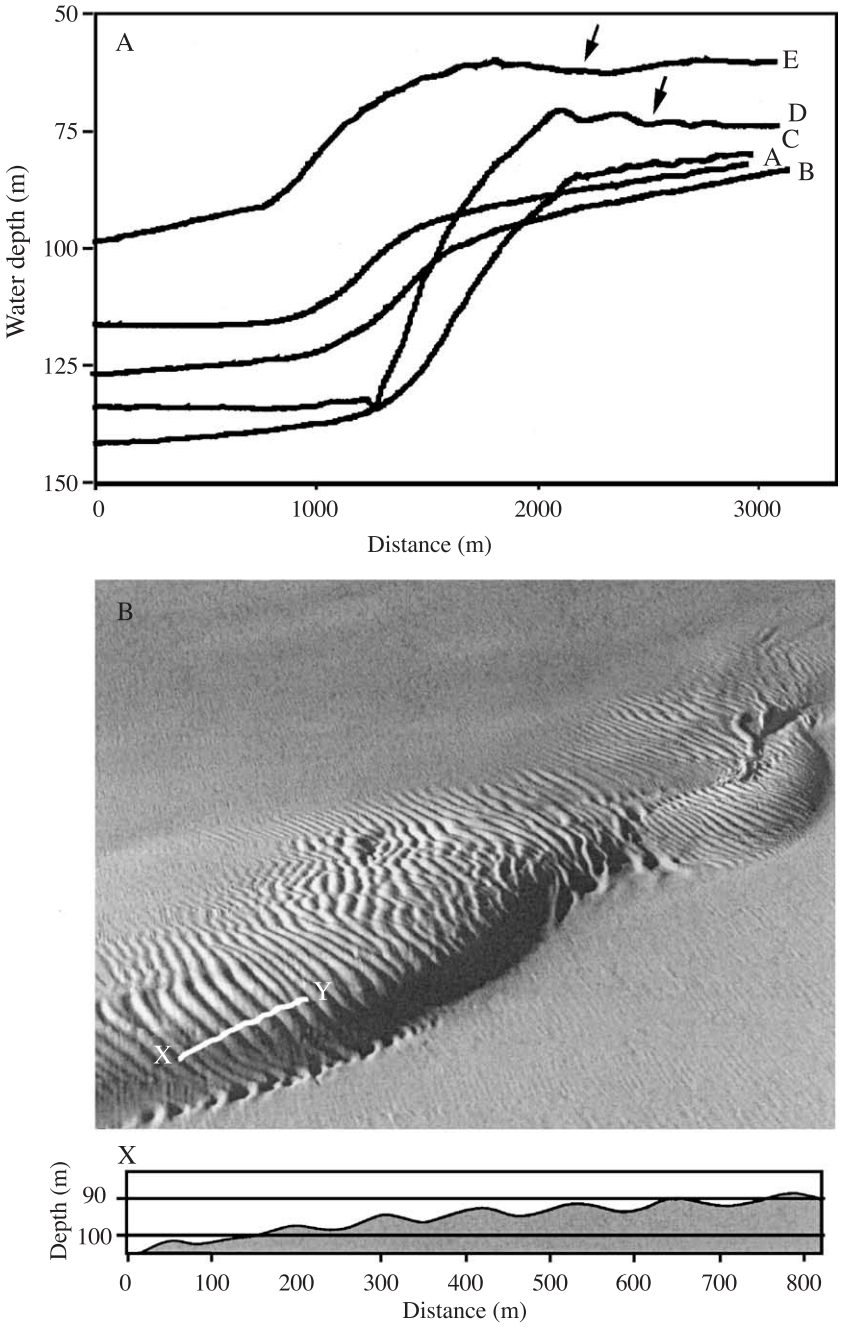

Fig. 14. (A) Bathymetric profiles across margin of Twin Ridges delta. Arrows point to moat behind delta rim. Locations of profiles A through E shown in Fig. 13B. (B) Perspective view of dune field, see location in Fig. 13B. Profile of bed forms from line XY shown below image.

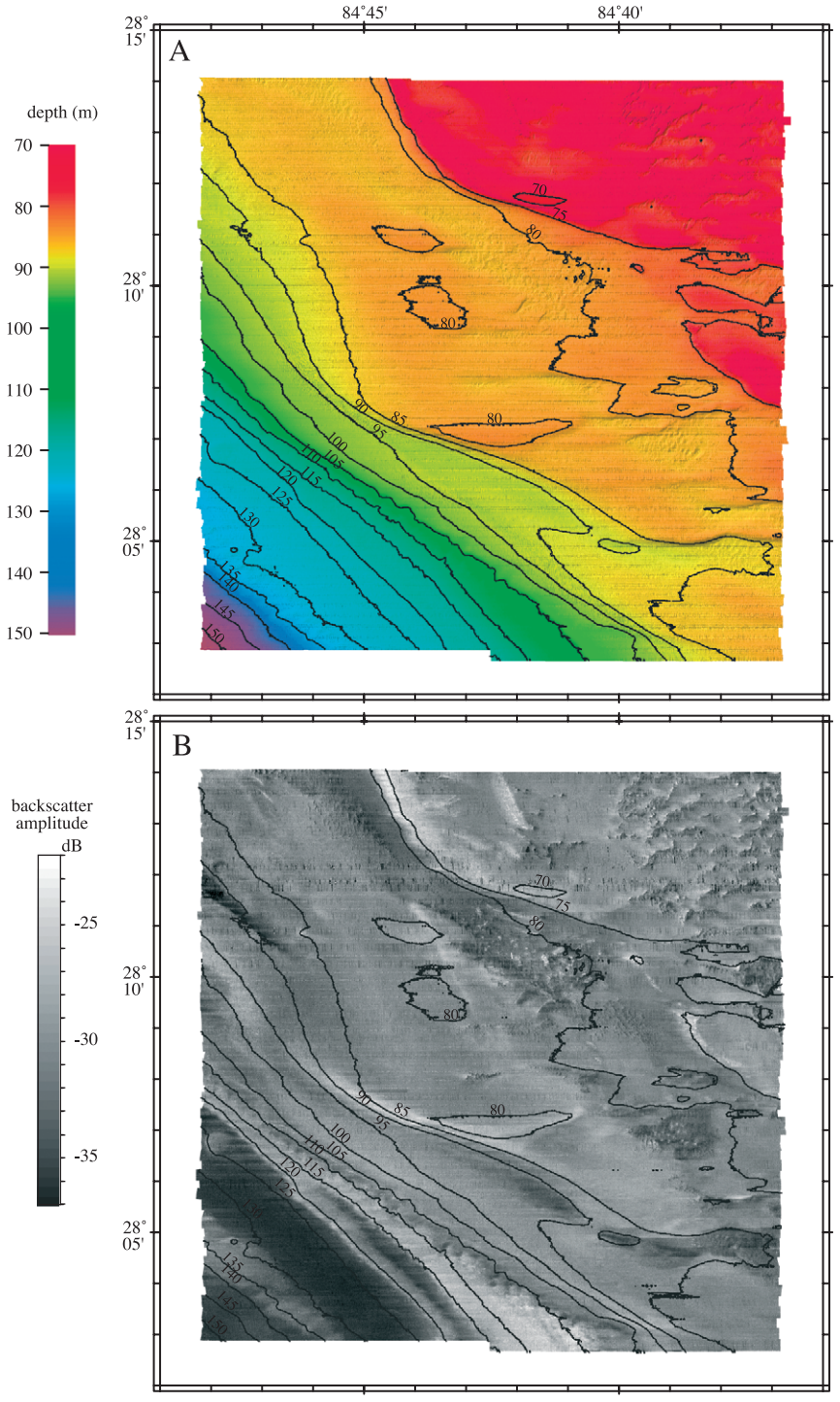

Fig. 15. (A) Color-shaded relief map view and (B) acoustic backscatter of Steamboat Lumps. Illumination for bathymetry from 315°, elevation is 45°.

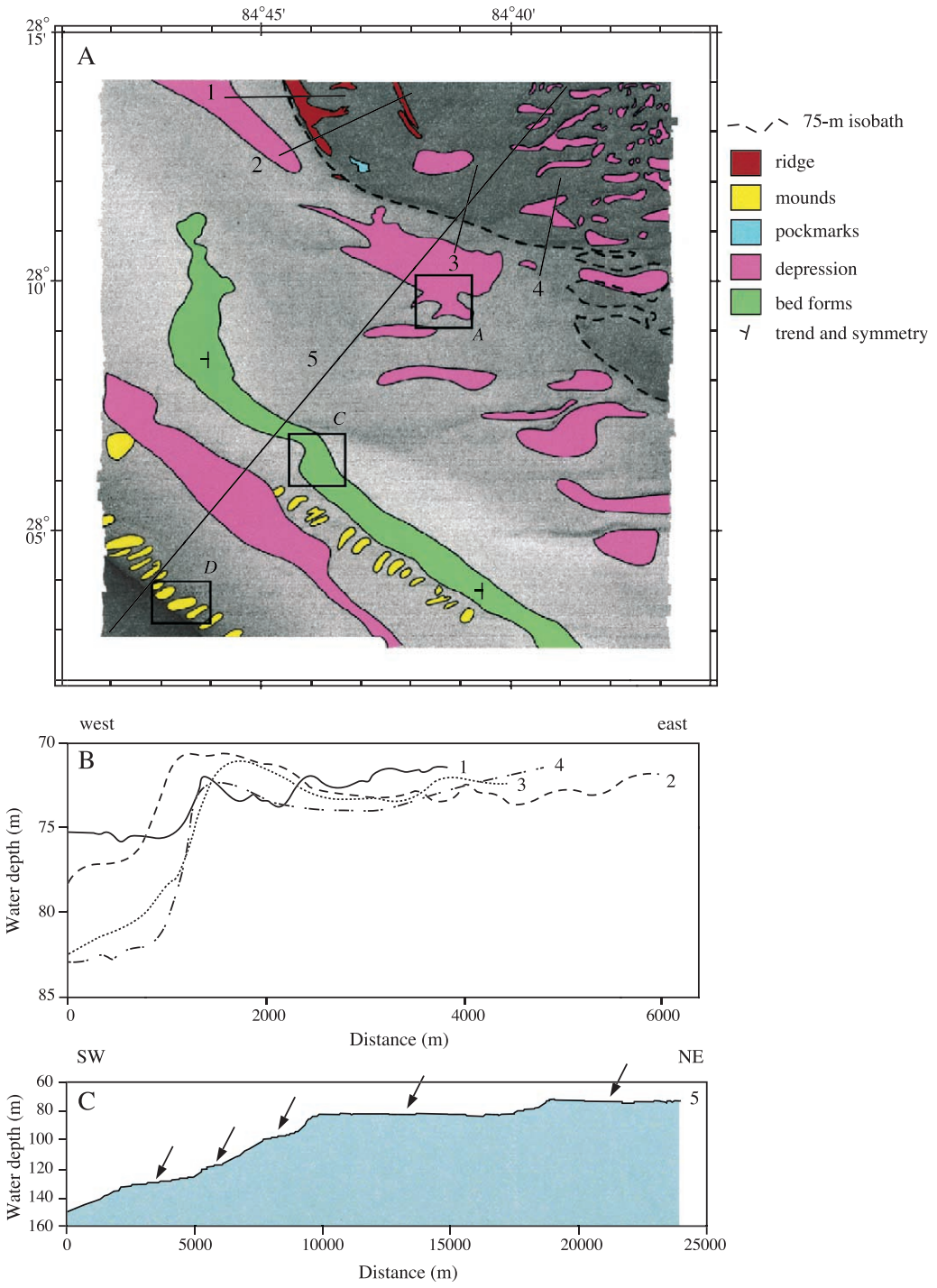

Fig. 16. Interpretation of features of Steamboat Lumps. Numbered lines correspond to profiles in (B), profile 5 shown in (C). Notice prevalence of raised platform rim in all profiles. Arrows in (C) point to terrace surfaces down the SW flank of Steamboat Lumps platform. See text for discussion.

bed forms range from 80 to 100 m in wavelength, 2 to 3 m in wave height, and are found in water depths that range from 65 to 130 m. The bed forms are asymmetric with the steepest sides facing the west along the southern margin veering to the NW along the SW margin.

2.1.7. Steamboat Lumps Reserve

Not enough of the Steamboat Lumps bathymetric feature was mapped to give it a geomorphic name. The Steamboat Lumps area is located 105 km SE of the Twin Ridges delta. The SW portion of Steamboat Lumps is composed of a series of five NW–SE-

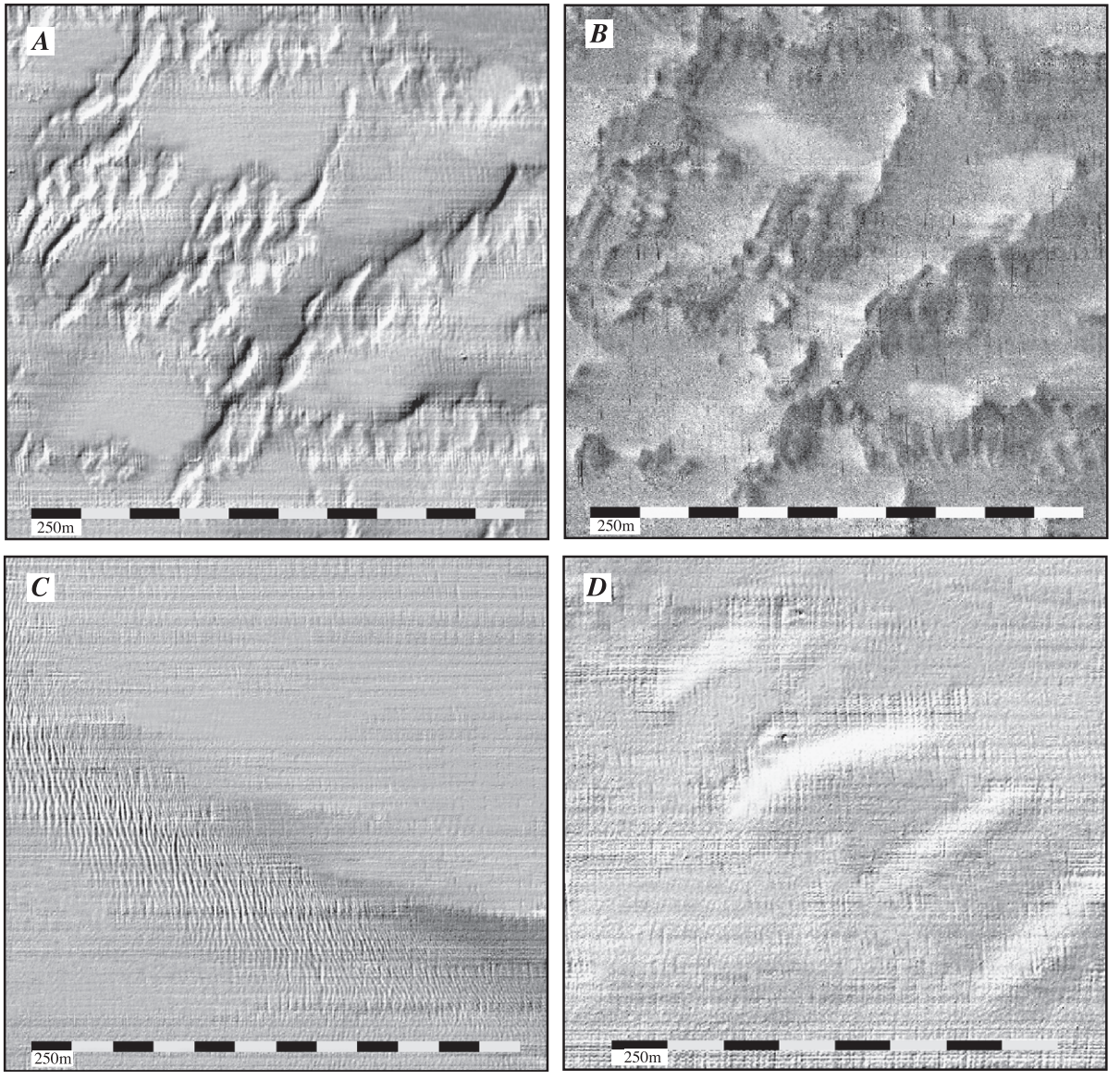

Fig. 17. (A) Bathymetry and (B) acoustic backscatter of depressions on SW flank of Steamboat Lumps. Depressions have lower backscatter than the surrounding surface. Illumination for bathymetry from 315°, elevation is 45°. (C) Bathymetry of field of asymmetric bed forms (steep side facing west) with 20- to 40-m wavelengths and wave heights of 0.2 to 0.5 m. (D) Bathymetry of mounds on SW flank of shallowest surface. Individual mounds have as much as 2 m of relief.

trending terraces stepped deeper toward the SW (Fig. 15). The shallowest terrace resembles the outer edge and slope of a delta, similar to those described to the north, and occupies the NE corner of the mapped area. This terrace is a relatively flat platform at water depths that vary only between 71 and 73 m. The edge of the platform trends NW–SE, and a pronounced rim with about 2 m of relief occurs all along the edge followed by a broad (~5 km) depression of about 1 m deep (Fig. 16B). The surface of the platform and its flank have a series of large depressions (Fig. 17) that range in relief from 0.5 to 1.0 m deep. The platform depressions have a distinctly lower acoustic backscatter compared to the surrounding areas. The margin of the 73-m platform is relatively steep (2.3°) along its entire length, with a step down to the west of about 7 m to the 80-m isobath. The 80-m terrace is 8 km wide and has a series of 1- to 2-m-deep depressions along its eastern area. These depressions have relatively high acoustic backscatter compared to the surrounding area. A small field of pockmarks is found on the outer edge of the terrace with a pockmark density of 66/km^2.

The next deepest terrace ranges in water depth from 92 to 98 m with a 0.5° tilt to the SW and is 700 m wide. Progressing SW, the next terrace is at depths of 115 to 118 m and is <50 m wide, followed by the last terrace at 123 to 130 m water depths and is 290 m wide. The terrace surfaces have relatively uniform intermediate acoustic backscatter values, but the slope between the 92- to 98-m terrace and the 115- to 118-m terrace is a band of high backscatter. Each terrace surface has depressions scattered throughout their extent (Fig. 16A). The floors of the depressions have irregular relief that in places resembles bed forms.

Two ridge segments are located on the shallowest terrace in water depths of 72 m. These ridges parallel the western rim of the terrace, but one ridge segment is located 3.6 km east of the rim, whereas the other is on the outer edge of the terrace. Both ridge segments stand 0.5 to 1.0 m in relief and are as much as 400 m wide. The ridges have moats immediately to their west, typically 0.5 m deep and about 20 m wide.

A large field of bed forms is located between the 89- and 99-m isobaths extending across almost the entire mapped area (Figs. 16 and 17C). The bed forms have wavelengths of 20 to 40 m and wave heights of 0.2 to 0.5 m. The bed forms are asymmetric with the steepest side facing W–NW, and the crests are short and slightly sinuous.

Two trends of mounds are found along the deeper terraces, one trend between the 105- to 117-m isobaths and the other between the 132- and 137-m isobaths (Figs. 16 and 17D). The mounds have as much as 2 m of relief and are elliptical in shape with major axes up to 1000 m long and minor axes up to 350 m long, with the major axis always trending directly downslope on a bearing of 060°.

3. Discussion

The physiographic features revealed by the multibeam data present three issues that require explanations: (1) what exactly do the shelf-edge platforms and the ridges represent, (2) when did these features form, and (3) how did the ridges built on the shelf projections survive the recent eustatic transgressions?

Two of the shelf projections, the Madison–Swanson and Twin Ridges deltas, are clearly shelf-edge deltas (McKeown et al., 2004). The similarity in morphology of the other four shelf projections mapped in this study to the two well-documented deltas studied by McKeown et al. (2004) strongly supports a shelf-edge origin for them as well. The deltas also superficially resemble deposits interpreted as low-stand deltas mapped along the shelf edge south of Texas (Winkler, 1982; Suter and Berryhill, 1985; Morton and Suter, 1996), on the Mississippi–Alabama shelf edge (Kindinger, 1988, 1989; Sydow and Roberts, 1994; Sager et al., 1999), and along the mid-Florida shelf edge (Jordan, 1951; Mitchum, 1978). These occurrences suggest that relict shelf-edge deltas are common along the outer continental shelf of the NE Gulf of Mexico. The deltas typically are composites of more than one lobe with one built upon another (Figs. 5, 9, 11, and 13). This suggests that the rivers that formed the deltas not only avulsed along the outer shelf but also were characterized by episodic flow with periods of nondeposition followed by renewed deposition. Locker and Doyle (1992) studied the inner shelf adjacent to the mapped area and identified a series of four late Pleistocene delta lobes that extend from immediately west of the De Soto Canyon along an easterly trend. The two easternmost of these inner-shelf delta lobes could be

the proximal portions of the Destin and 29-40 deltas. Acoustic backscatter of the delta surfaces is higher than the adjacent shelf-ramp areas. The backscatter intensity, assuming it is a response to sediment facies only (i.e., no bed roughness or volume reverberation), suggests that the relict deltas are mantled with sediment with acoustic properties in the range of coarse silt to medium sand, whereas the surrounding shelf-ramp areas are covered by fine to coarse silt (Table 3). Sediment studies suggest that the entire region, with the exception of the immediate area of the Destin delta, is draped with the MAFLA quartz sand sheet (Doyle and Sparks, 1980; Mazzulo and Peterson, 1989), a facies that is consistent with the acoustic backscatter. The area of the Destin delta is composed of shell hash, *Lithothamnion* algae, and foraminifera, with carbonate percentages in excess of 75% (Doyle and Sparks, 1980). This carbonate facies may be represented by the 400-m-wide high-backscatter halo that surrounds the ridges on the Destin delta.

As pointed out by McKeown et al. (2004), the proximity of the Apalachicola River delta and associated barrier islands <50 km to the NE suggests that the river was the major source for the delta sediments. Other rivers of the panhandle of Florida (Perdido, Escambia, Blackwater, and Yellow Rivers) and Alabama (Pascagoula River) also formed deltas during lower stands of sea level (Bart and Anderson, 2004). The restricted range of water depths of the delta surfaces (−55 to −85 m) suggests that the deltas are not the often interpreted *low-stand* delta lobes, because the depth range of the delta surfaces does not correspond to a period of a eustatic low-stand. The deltas could not have formed during the low-stands that occurred from 23 to 16 ka and 145 to 130 ka, because sea level at that time was at about the 120-m isobath placing the locations of the deltas >35 m *above* sea level. Likewise, the deltas could not have formed during the brief regression of the Younger Dryas (11,000 to 10,000 yBP), because sea level stood above the present 50-m isobath during that time. This leaves three models, assuming deposition during the last 130,000 years, when sea level stood at depths that would allow the construction of the deltas and ridges. The first scenario is that the deltas formed during a brief still stand that interrupted the rapid transgression of Marine Isotope Stage (MIS)6-5 or the MIS2-1. Detailed sea level curves for MIS6-5 are rare (i.e., Chappell et al., 1996), but most detailed sea level curves for the MIS2-1 transgression show two steps (Fairbanks, 1989) or three steps (Blanchon and Shaw, 1995) in sea level rise. However, each step does not represent a stasis in the transgression but rather an order-of-magnitude increase in the already rapid rate of sea level rise. The timing of the first sudden rise (melt water pulse MWP-1A) occurred when almost NW Florida outer shelf was subaerial by ~20 m (Fig. 18). The timing of the second sudden rise (MWP-1B) puts sea level at about 53 to 50 m below present sea level, when the NW Florida outer shelf was already ~20 m below sea level (Fairbanks, 1989; Hanebuth et al., 2000). In addition, a stasis in the transgression of some duration would be required to construct first the large deltas and then the ridges on their surfaces. Therefore, this scenario seems unlikely to be valid. The three intervals of rapid sea level rise or fall represent only very short windows of time (perhaps a few hundred years) to develop shelf-edge deltas.

The second scenario is that the deltas formed sometime during the end of the rapid regression at the MIS5-4 transition and/or the early stages of MIS04 (Fig. 18). This is a period of almost 10,000 years when sea level stood at a depth of the 29-20, 29-40, and Twin Ridges deltas. However, the Destin delta at this time would have been subaerial by ~ 20 m, and the Madison–Swanson delta would have been submerged by ~20 m. Nevertheless, the 29-20, 29-40, and Twin Ridges deltas could have formed during this period.

The third and more likely interpretation is that the deltas formed during a prolonged period of relative

Table 3
Range of 100-kHz acoustic backscatter (BS) for different facies, assuming all of backscatter energy is derived from the grain size with no contribution from bed roughness or volume reverberation (after Jackson, 1994)

Facies	High BS (dB)	Low BS (dB)
Rough rock	−4.0	−9.0
Rock	−7.0	−12.0
Cobble	−12.0	−16.0
Sandy gravel	−14.5	−20.0
Coarse sand	−14.5	−23.0
Medium sand	−17.0	−25.0
Very fine sand	−22.5	−27.5
Coarse silt	−27.0	−32.0
Fine silt	−32.0	−38.0

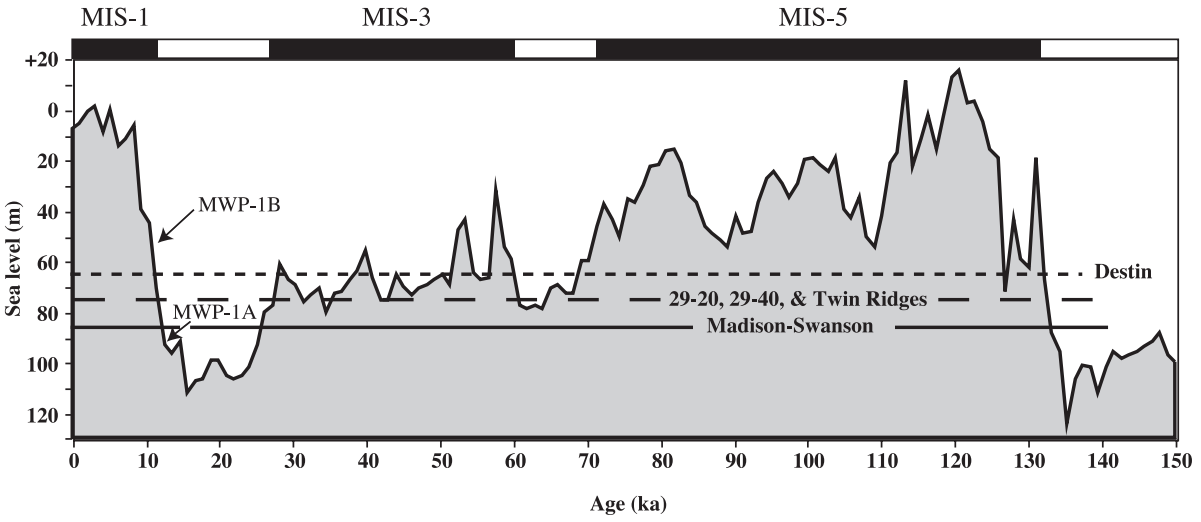

Fig. 18. Sea-level curve for the last 150,000 years derived from Pillans et al. (1998). Bar at top is Marine Isotope Stages after Martinson et al. (1987). Short dashed line is depth of Destin delta; long dashed line is depth 29-20, 29-40, and Twin Ridges deltas, and solid line is depth of Madison–Swanson delta.

sea-level stasis, such as occurred during the 35,000 years of MIS-3 (Fig. 18). This interval of relatively constant or gradually falling sea levels provides ample time for large deltas to have developed and for the ridges to have been constructed on their surfaces. Although the surfaces of Destin, 29-20, 29-40, and Twin Ridges deltas all fall close to the MIS-3 portion of the sea level curve, the Madison–Swanson delta would have formed at depths of ~10 m below sea level. Given the uncertainty in the sea level curve, as well as the effects of compaction and sediment loading on the outer shelf, the correlation seems justified. Consequently, the model that best fits the bathymetric data is the one in which the deltas formed during the long period of relative stasis or slow marine regression prior to the last glacial period. However, the construction and preservation of the ridges must also be considered before a most likely model can be accepted.

The ridges constructed on the delta surfaces superficially resemble both biogenic barrier reefs as well as barrier islands. The ridges have much higher acoustic backscatter than the surrounding seafloor (Table 1), and the range of backscatter suggests (again assuming no contribution from bed roughness and volume reverberation) that the acoustic properties of the ridge materials resemble sandy gravel to medium sand (Table 3). Barrier reefs typically have a platform, a shoreface with spur and groove structure, a reef front, and a back-reef lagoon (Guilcher, 1988). A barrier island complex is typically composed of six elements: the mainland, a back-barrier lagoon, tidal inlets and tidal deltas, the barrier island, a barrier platform, and a shoreface (Oertel, 1985). The main morphological differences between a biogenic reef and a barrier island are the slope of the seaward-facing edge of the feature. A reef should rise at angles above the 25° to 30° angle of repose (Guilcher, 1988), whereas a barrier island should have a seaward-facing equilibrium profile with gradients of only a few degrees, much less than the angle of repose (Swift et al., 1985). The ridges have seaward-facing slopes of only a few degrees and do not approach 20°. In other morphologic parameters, such as length-to-width ratios, heights, and associated features, such as back-ridge lagoons and passes, both biogenic reefs and barrier islands are superficially quite similar. However, two features strongly support the barrier island interpretation for the ridges. The first is a zone of numerous low-standing, slightly curved ridges that occur behind (landward) both the 29-40 and 29-20 deltas (Fig. 6F). These ridges resemble in virtually all respects the beach-ridge terraces found on the strand plain, such as those of the Cape San Blas area off the Apalachicola River (Otvos, 1992) and off the Doce River of Brazil (Dominguez and Wanless, 1991).

These strandplain ridges have been described as a result of sedimentation during a minor sea-level regression (Thom, 1983; Boyd et al., 1992). The second feature is the seaward-facing slopes of all of the ridges, except Destin Ridge, have gradients of <10° and in most places are only a degree or two (Table 2).

The available literature does not mention coral reef debris in the surficial sediments off NW Florida. However, the most extensive sediment analysis describes the typical sediment as a marl or chalk with "... 55% fragmental debris" (Ludwick, 1964, p. 226). Doyle and Sparks (1980) described a carbonate-rich facies (although they did not mention coral debris) restricted to the area of the Destin delta. Coral debris was described in the surficial sediments from similar water depths on the Alabama–Mississippi outer continental shelf (Ludwick and Walton, 1957), hence it would not be surprising to find coral reefs at this latitude on the NW Florida shelf. Briere et al. (1999) provides general qualitative descriptions of a few sediment samples from the western Florida shelf, and a few descriptions mention "coral debris". However, those samples are far to the SE of the study area.

Coral reefs typically, although not exclusively, develop in areas with little sediment input to the immediate offshore. Sediment, especially fine-grained sediment, tends to smother corals and either stunts or buries them. Barrier islands, on the other hand, require a ready supply of sediment, provided by longshore drift and/or the adjacent shelf. The Apalachicola River, although not major by world standards, is the largest river of the panhandle of Florida, and it has built a delta and a series of barrier islands during the present high stand (Otvos, 1992; Fig. 19). The river is thought to have been a significant river during the Pleistocene (Otvos, 1992). The ages of the barrier islands clearly postdate the formation of the delta they sit on. Consequently, the issues are not the sediment supplies necessary to construct the barrier islands or their ages, but rather how could the barrier islands survive a marine transgression.

The preservation potential of a siliciclastic feature such as a barrier island is sensitive to the sign of sea-level change (Davis and Clifton, 1987; Field and Trincardi, 1991). Relict eolian dunes, beach ridges, mud ridges, and mud wedges are conventionally interpreted to have been formed and then drowned during the rapid marine transgression of the last deglaciation (i.e., Locker et al., 1996; Liu et al., 2002; Chen et al., 2003). Most of these observations have been made off high-energy coasts adjacent to major rivers with huge sediment loadings. However, the NE Gulf of Mexico is a low-energy environment, and the rivers in this area transport only modest sediment loads. A slow transgression would effectively bulldoze a young barrier island and create a sand shoal not drown the barrier intact (Swift et al., 1985; Davis and Clifton, 1987). However, a rapid marine transgression, such as that which occurred during the last deglaciation (MIS-2/1), potentially could have effectively drowned a barrier island with only minor destruction. As discussed above, the last transgression was very rapid with no identifiable stillstands. But there had to be sufficient time during a sea-level stillstand to allow the barrier islands and strandplain beach ridges to form. A more plausible explanation for the preservation of the barrier islands is that they formed during a relatively long period of sea-level stasis or slow regression. A period of sea-level stasis, similar to the Holocene, would have created the conditions necessary to construct and perhaps partially cement the barrier island by subaerial processes; and a slow regression would have allowed strandplain beach ridges to form. The last major regression began about 58,000 years ago during early MIS-3 (Fig. 18). Eustatic sea level fluctuated ±10 m about a steady decrease that dropped from 51 to 75 m (mean of 66 m) over a 30,000-year interval, giving a mean sea-level regression of 0.8 m/ky (Chappell et al., 1996; Pillans et al., 1998; Cutler et al., 2003). The regression was not monotonic, but rather was a series of small sea level rises and falls. Consequently, the only time during the last 150,000 years that sea level was at the depth of the barrier islands and was in a regressive state was during MIS-3, the same interval suggested for the development of the delta lobes.

The Coral Trees ridges do not resemble the ridges interpreted as barrier islands. Geomorphically, the Coral Trees ridges are rough-topped, short, en echelon segments (Fig. 8D). The north Coral Trees ridges strike at an angle to the isobaths, whereas the south Coral Trees ridges parallel the isobaths. Both sets of ridges occur not on the delta lobes but on the

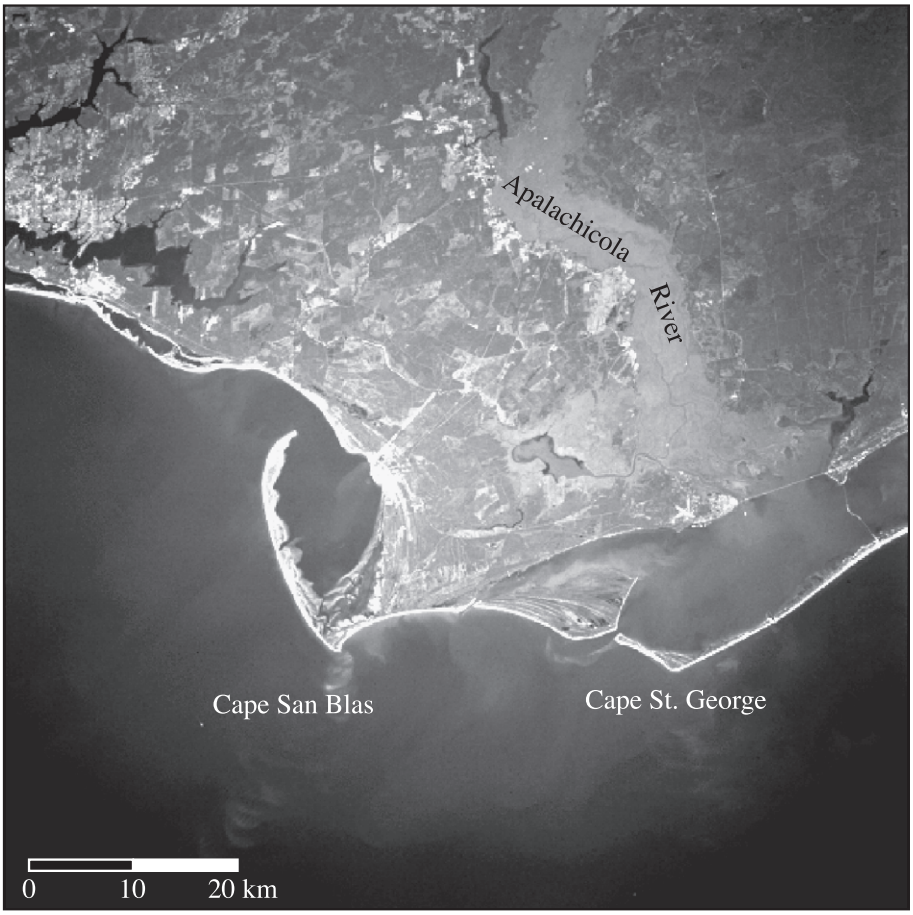

Fig. 19. Satellite photograph of the Cape San Blas–Cape St. George barrier islands immediately offshore the Apalachicola River, Florida. Note the resemblance of the barrier island plans to that of the 29-40 and 29-20 barrier islands (Figs. 5 and 9, respectively).

sediment ramps between the delta lobes in water depths that range from 88 and 95 m. The mounds found in the Coral Trees area, as well as those adjacent to Destin delta, and on the 29-40, 29-20, and Madison–Swanson delta lobes are smooth, elongated features that typically occur in water depths deeper than 100 m. Not enough information is available to make anything but a speculation about what these features might represent. One possibility is that both the Coral Trees ridges and the mounds are *Oculina* lithoherms. *Oculina* is a relatively deep–water ahermatypic coral that lacks zooxanthellae and forms coral thickets that trap sediment and coral debris into mounds, often capped with live coral (Reed, 2002).

With the exception of Coral Trees ridges, all of the inferred barrier islands were constructed on the south and west side of the shelf-edge deltas. This preference suggests that the prevailing winds were southerlies and southwesterlies, because barrier islands typically face into the prevailing winds. Fields of bed forms occur on the delta surfaces as well as on their south and SW flanks. The bed form crests on the delta surfaces are aligned S–SE and are asymmetrical with the steepest side facing north, suggesting a northward-flowing current. Large bed forms, properly called dunes in the terminology of Ashley (1990), are found along the southern and SW margins of the deltas, but the crests of these bed forms are aligned perpendicular to the contours with

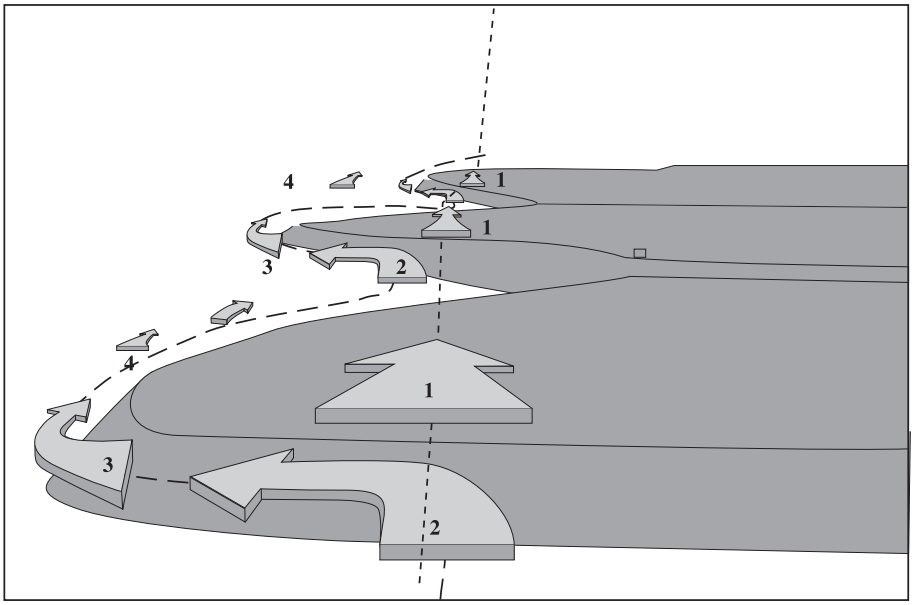

Fig. 20. Cartoon oblique view of delta lobes and current flows. Number 1 indicates the current flow across the tops of the delta lobes. This flow was sufficient to form dunes on the delta surfaces. Number 2 indicates the current splitting and accelerating as it encounters the flanks of the delta lobes. This is the zone with the well-developed dunes. Number 3 shows the geostrophic flow steering around the front of the delta lobes and slowing. The current speed is still sufficient to form dunes. Number 4 shows the flow slowing to the point where it does not form bed forms and continuing until it encountered the next delta lobe.

steepest sides facing west (south slopes) and NW (SW slopes). The alignment of the delta-margin dunes suggests a strong geostrophic flow from the south that was steered by the relief of the delta lobes. The current appears to have accelerated as it flowed around each delta and then slowed in the cul-de-sacs between the deltas (Fig. 20). The bed forms on the delta surfaces indicate that the geostrophic flow was sheered into two flows by the presence of the delta topography; the upper section of the flow continued its northward flow uninterrupted, while the lower section of the flow was steered around each delta margin. Although many of the hurricanes that periodically pass over the area are capable of reworking the bottom at the present depths of the delta-surface bed forms, the predominate location of the bed form fields on the south side of the delta surfaces, as well as the consistent bed form asymmetry pointing to a northerly flow, suggests that these bed forms are the result of an unidirectional flow and not of omnidirectional confusion that would be expected from periodic hurricanes.

4. Conclusions

The geomorphology of the NW Florida continental shelf is much more complicated than the published literature would suggest. The area east of the De Soto Canyon is characterized by at least six shelf-edge deltas that project southwestward from the 55-m isobath. The deltas were constructed on the mid- and outer shelf when sea level ranged between −55 to −85 m during a period of slow regression spanning 35,000 years of MIS-3. The deltas are composite features suggesting the rivers that built them avulsed back and forth across the broad mid- to outer-shelf region, consistent with the sea-level oscillations of MIS-3.

Each of the deltas has a barrier–island complex preserved on its south and SW margins. The barrier–island complexes range in morphology from simple linear ridges (Destin and Madison–Swanson deltas) to an intricate assemblage of features that include barrier island, strandplains beach ridges, and inlets (29-20 and 29-40 deltas).

Large slope-perpendicular dunes are found along the southern and SW slopes of the deltas, and smaller east–west-trending bed forms are found on the southern and SW surfaces of the deltas. The asymmetry of the bed forms suggests a strong geostrophic subsurface current flowed from south to north but was sheered by the presence of the shelf-edge deltas, separating into a steered flow around the deltas and a continuous flow across the surfaces of the deltas. The age of the bed forms is unknown, but no northward-flowing geostrophic flow is found in this area today.

Hopefully, this mapping will lead to ground truthing these features, a necessary next step to determine the true nature and age of the deltas, barrier–island complexes, and bed forms. A critically important target for the next stage of this research is determining the nature of sediment supply and bottom-water circulation patterns that controlled the formation of these features.

Acknowledgements

We would like to acknowledge the efforts by the C & C Technologies crew, especially, Art Kleiner, Dave Fitts, Wes Kitt, Ryan Larson, and Heather Carnocki, aboard RV *Moana Wave* during this cruise. The data quality for this study is a tribute to their professionalism. Earlier versions of the manuscript were significantly improved by constructive comments by Bob Morton, John Anderson, Ron Boyd, and Eric Grossman. The cruise was an outgrowth of a partnership between the U.S. Geological Survey, Minerals Management Service, and the National Marine Fisheries Service and was conducted under cooperative agreements between the USGS and the Universities of New Hampshire and New Brunswick (Canada). We acknowledge the support of Mike Carr, Ken Sulak, and Gary Brewer (USGS), Tom Ahlfeld (MMS), and Andrew David (NMFS). Any use of trade names does not constitute an endorsement by the USGS, MMS, NMFS, or the U.S. Government.

References

Ashley, G.M., 1990. Classification of large-scale subaqueous bed forms: a new look at an old problem. Journal of Sedimentary Petrology 60, 160–172.

Ballard, R.D., Uchupi, E., 1970. Morphology and Quaternary history of the continental shelf of the Gulf Coast of the United States. Bulletin of Marine Science 20, 547–559.

Bart, P.J., Anderson, J.B., 2004. Late Quaternary stratigraphic evolution of the Alabama–west Florida outer continental shelf. In: Anderson, J.B., Fillon, R. (Eds.), Late Quaternary Stratigraphic Evolution of the Northern Gulf of Mexico, Society of Economic Paleontologists and Mineralogists Special Publication 79.

Blanchon, P., Shaw, J., 1995. Reef drowning during the last deglaciation: evidence for catastrophic sea-level rise and ice-sheet collapse. Geology 23, 4–8.

Boyd, R., Dalrymple, R., Zaitlin, B.A., 1992. Classification of clastic oastal depositional environments. Sedimentary Geology 80, 139–150.

Briere, P.R., Scanlon K.M., Fitzhugh, Gary, Gledhill, C.T., Koenig C.C., 1999. West Florida shelf: sidescan-sonar and sediment data from shelf-edge habitats in the northeastern Gulf of Mexico. U.S. Geological Survey Open-file Report 99-589. CD-ROM.

Chappell, J., Omura, A., Esat, T., McCulloch, M., Pandolfi, J., Ota, Y., Pillans, B., 1996. Reconciliation of late Quaternary sea levels derived from coral terraces at Huon Peninsula with deep sea oxygen isotope records. Earth and Planetary Science Letters 141, 227–236.

Chen, Z., Saito, Y., Hori, K., Zhao, Y., Kitamura, A., 2003. Early Holocene mud–ridge formation in the Yangtze offshore, China: a tidal-controlled estuarine pattern and sea-level implications. Marine Geology 198, 245–257.

Cutler, K.B., Edwards, R.L., Taylor, F.W., Cheng, H., Adkins, J., Gallup, C.D., Cutler, P.M., Burr, G.S., Bloom, A.L., 2003. Rapid sea-level fall and deep-ocean temperature change since the last interglacial period. Earth and Planetary Science Letters 206, 253–271.

Davis Jr., R.A., Clifton, H.E., 1987. Sea-level change and the preservation potential of wave-dominated and tide-dominated sequences. In: Nummendal, D., Pilkey, O.H., Howard, J.D. (Eds.), Sea-level Fluctuation and Coastal Evolution, Society of Economic Paleontologists and Mineralogists Special Publication vol. 41. , pp. 167–178.

Dominguez, J.M.L., Wanless, H.R., 1991. Facies architecture of a falling sea-level strandplain, Doce River, Brazil. In: Swift, D.J.P., Oertel, G.F., Tillman, R.W., Thorne, J.A. (Eds.), Shelf Sand and Sandstone Bodies, Geometry, Facies and Sequence Stratigraphy, Special Publication, vol. 14. International Association of Sedimentologists, pp. 259–281.

Donoghue, J.F., 1993. Late Wisconsinan and Holocene depositional history, northeastern Gulf of Mexico. Marine Geology 112, 185–205.

Doyle, L.J., Sparks, T.N., 1980. Sediments on the Mississippi, Alabama, and Florida (MAFLA) continental shelf. Journal of Sedimentary Petrology 50, 905–915.

Fairbanks, R.G., 1989. A 17,000-year glacio-eustatic sea level record: influence of glacial melting rates on the Younger Dryas event and deep-ocean circulation. Nature 342, 637–642.

Field, M.E., Trincardi, F., 1991. Regressive coastal deposits on Quaternary continental shelves: preservation and legacy. In:

Osborne, R.H. (Ed.), From Shoreline to Abyss: Contributions in Marine Geology in Honor of Francis Parker Shepard, Society for Sedimentary Geology Special Publication, vol. 46, pp. 107–122.

Gardner, J.V., Mayer, L.A., Hughes Clarke, J.E., Kleiner, A., 1998. High-resolution multibeam bathymetry of East and West Flower Gardens and Stetson Banks, Gulf of Mexico. Gulf of Mexico Science 16, 131–143.

Gardner, J.V., Dartnell, P., Sulak, K.J., Calder, B.R., Hellequuin, L., 2001. Physiography and late Quaternary–Holocene processes of northeastern Gulf of Mexico outer continental shelf off Mississippi and Alabama. Gulf of Mexico Science 18, 132–157.

Gardner, J.V., Dartnell, P., Sulak, K.J., 2002. Multibeam mapping of the west Florida shelf, Gulf of Mexico. U.S. Geological Survey Open-File Report, OF02-5.

Guilcher, A., 1988. Coral Reef Geomorphology. John Wiley and Sons, New York. 288 pp.

Hanebuth, T., Stattegger, K., Grootes, P.M., 2000. Rapid flooding of the Sunda shelf: a late-glacial sea-level record. Science 288, 1033–1035.

Hughes Clarke, J.E., 2000. Present-day methods of depth measurement. In: Cook, P.J., Carleton, C.M. (Eds.), Continental Shelf Limits: The Scientific and Legal Interface. Oxford Univ. Press, New York, pp. 139–159.

Hughes Clarke, J.E., Mayer, L.A., Wells, D.E., 1996. Shallow-water imaging multibeam sonars: a new tool for investigating seafloor processes in the coastal zone and on the continental shelf. Marine Geophysical Research 18, 607.

Jackson, D.R., 1994. APL-UW high-frequency ocean environmental acoustic models handbook, Technical Report APL-UW TR9407, 195 pp.

Jordan, G.F., 1951. Continental slope off Apalachicola River, Florida. Bulletin of the American Association of Petroleum Geologists 35, 1978–1993.

Kindinger, J.L., 1988. Seismic stratigraphy of the Mississippi–Alabama shelf and upper continental slope. Marine Geology 83, 79–94.

Kindinger, J.L., 1989. Depositional history of the Lagniappe Delta, northern Gulf of Mexico. Geo-Marine Letters 9, 59–66.

Koenig, C.C., Coleman, F.C., Grimes, C.B., Fitzhugh, G.R., Scanlon, K.M., Gledhill, C.T., Grace, M., 2000. Protection of fish spawning habitat for the conservation of warm temperate reef fish fisheries of shelf-edge reefs of Florida. Bulletin of Marine Science 66, 593–616.

Liu, J.P., Milliman, J.D., Gao, S., 2002. The Shandong mud wedge and post-glacial sediment accumulation in the Yellow Sea. Geo-Marine Letters 21, 212–218.

Locker, S.D., Doyle, L.J., 1992. Neogene to Recent stratigraphy and depositional regimes of the northwest Florida inner continental shelf. Marine Geology 104, 123–138.

Locker, S.D., Hine, A.C., Tedesco, L.P., Shinn, E.A., 1996. Magnitude and timing of episodic sea-level rise during the last deglaciation. Geology 24, 827–830.

Ludwick, J.C., 1964. Sediments in northeastern Gulf of Mexico. In: Miller, R.L. (Ed.), Papers in Marine Geology, Shepard Commemorative Volume. The Macmillan Co., New York, pp. 204–238.

Ludwick, J.C., Walton, W.R., 1957. Shelf-edge calcareous prominences in northeastern Gulf of Mexico. American Association of Petroleum Geologists Bulletin 41, 2054–2101.

Martinson, D.G., Pisias, N.G., Hayes, J.D., Imbrie, J., Moore Jr., T.C., Shackleton, N.J., 1987. Age dating and the orbital theory of the ice ages: development of a high-resolution 0 to 300,000-year chronostratigraphy. Quaternary Research 27, 1–29.

Mazzulo, J., Peterson, M., 1989. Sources and dispersal of late Quaternary silt on the northern Gulf of Mexico continental shelf. Marine Geology 86, 15–26.

McBride, R.A., Byrnes, M.R., 1995. Surficial sediments and morphology of the southwestern Alabama/western Florida Panhandle coast and shelf. Gulf Coast Association of Geological Societies Transactions, vol. 45, pp. 392–404.

McKeown, H.A., Bart, P.J., Anderson, J.B., 2004. High resolution stratigraphy of a sandy, ramp-type margin-Apalachicola, Florida. In: Anderson, J.B., Fillon, R. (Eds.), Late Quaternary Stratigraphic Evolution of the Northern Gulf of Mexico, Society of Economic Paleontologists and Mineralogists Special Publication 79.

Mitchum Jr., R.M., 1978. Seismic stratigraphic investigation of west Florida slope, Gulf of Mexico, Framework, facies, and oil-trapping characteristics of the upper continental margin. In: Bouma, A.H., Moore, G.T., Coleman, J.M. (Eds.), American Association of Petroleum Geologists, Studies in Geology, vol. 7, pp. 193–223.

Molinari, R.L., Mayer, D.A., 1982. Current meter observations on the continental slope at two sites in the eastern Gulf of Mexico. Journal of Physical Oceanography 12, 480–484.

Morton, R.A., Suter, J.R., 1996. Sequence stratigraphy and composition of Late Quaternary shelf-margin deltas, northern Gulf of Mexico. American Association of Petroleum Geologists Bulletin 80, 505–530.

Oertel, G.F., 1985. The barrier island system. Marine Geology 63, 1–18.

Otvos, E.G., 1992. Quaternary evolution of the Apalachicola coast, northeastern Gulf of Mexico, Quaternary coasts of the United States: Marine and lacustrine systems. Society of Economic Paleontologists and Mineralogists Special Publication 48, 221–232.

Pillans, B., Chappell, J., Nash, T.R., 1998. A review of the Milankovitch climatic beat: template for Plio-Pleistocene sea-level changes and sequence stratigraphy. Sedimentary Geology 122, 5–21.

Reed, J.K., 2002. Comparison of deep-water coral reefs and lithotherms off southeastern USA. In: Watling, L., Risk, M. (Eds.), Biology of Cold Water Corals, Hydrobiologia, vol. 471, pp. 57–69.

Sager, W.W., Schroeder, W.W., Davis, K.S., Rezak, R., 1999. A tale of two deltas: seismic mapping of near surface sediments on the Mississippi–Alabama outer shelf and implications for recent sea level fluctuations. Marine Geology 160, 119–136.

Scanlon, K.M., Koenig, C.C., Coleman, F.C., Rozycki, J.E., 2001. Paleoshorelines, drowned reefs, and grouper habitat in the

northeastern Gulf of Mexico. Geological Association of Canada Annual Meeting 26, 132. (abstracts).

Suter, J.R., Berryhill, H.L., 1985. Late Quaternary shelf-margin deltas, northwest Gulf of Mexico. American Association of Petroleum Geologists Bulletin 69, 77–91.

Swift, D.J.P., Niederoda, A.W., Vincent, C.E., Hopkins, T.S., 1985. Barrier island evolution, middle Atlantic shelf, USA, Part 1: Shoreface dynamics. Marine Geology 63, 331–361.

Sydow, J.C., Roberts, H.H., 1994. Stratigraphic framework of a Late Pleistocene shelf edge delta, northeast Gulf of Mexico. American Association of Petroleum Geologists Bulletin 78, 1276–1312.

Thom, B.G., 1983. Transgressive and regressive stratigraphies of coastal sand barriers in southeast Australia. Marine Geology 56, 137–158.

Vokovich, F.M., 1988. Loop Current boundary variations. Journal of Geophysial Research 93, 15,585–15,591.

Winkler, C.D., 1982. Cenozoic shelf margins, northwest Gulf of Mexico. Gulf Coast Association of Geological Societies Transactions 32, 427–448.